REPORT SERIES IN AEROSOL SCIENCE
N:o 137 (2012)

DYNAMICS OF NEUTRAL AND CHARGED AEROSOL PARTICLES

JOHANNES LEPPÄ

Finnish Meteorological Institute
Climate Change
Helsinki, Finland

Academic dissertation

To be presented, with the permission of the Faculty of Science of the University of Helsinki, for public criticism in auditorium D101, Gustaf Hällströmin katu 2, on November 23rd, 2012, at 12 o'clock noon.

Helsinki 2012

Author's Address: Finnish Meteorological Institute
P.O. Box 503
FI-00101 Helsinki
johannes.leppa@fmi.fi

Supervisors: Professor Veli-Matti Kerminen, Ph.D.
Department of Physics
University of Helsinki

Professor Markku Kulmala, Ph.D.
Department of Physics
University of Helsinki

Docent Lauri Laakso, Ph.D.
Climate Change
Finnish Meteorological Institute

Professor Kari E. J. Lehtinen, Ph.D.
Department of Applied Physics
University of Eastern Finland

Reviewers: Docent Sami Romakkaniemi, Ph.D.
University of Eastern Finland

Peter Tunved, Ph.D.
Stockholm University

Opponent: Professor Jyrki Mäkelä, Ph.D.
Technical University of Tampere

ISBN 978-952-5822-66-3 (printed version)
ISSN 0784-3496
Helsinki 2012
Unigrafia Oy

ISBN 978-952-5822-67-0 (PDF version)
http://ethesis.helsinki.fi/
Helsinki 2012
Helsingin yliopiston verkkojulkaisut

Acknowledgements

The research of this thesis has been conducted at the Aerosols and Climate Group, Climate Change Unit, Research and Development Division of the Finnish Meteorological Institute. I would like to thank the institute, especially the head of the division, Prof. Yrjö Viisanen, and unit leaders, Prof. Ari Laaksonen and Prof. Heikki Järvinen, for providing the working facilities and resources needed for this work. I would also like to thank the group leader, Doc. Heikki Lihavainen, for providing me help whenever it was needed and, especially, for allowing me to be part of such a great group. I would like to express my gratitude to the whole group for the friendly and supportive working atmosphere.

I would like to thank my supervisors, Prof. Veli-Matti Kerminen, Prof. Markku Kulmala, Doc. Lauri Laakso and Prof. Kari Lehtinen, without whom this research would not have been possible. Prof. Kerminen has provided me invaluable guidance on all of the aspects related to scientific work and it has been an utmost privilege to work with him. Prof. Kulmala gave me the initial opportunity to work in the field of aerosol science and has been guiding my work ever since. Doc. Laakso has provided me valuable information on air ions and atmospheric measurements as well as made sure that my work did not stall due to too much pondering. Prof. Lehtinen has helped me with the analytical part of this work and given excellent advices on emphasising the most important results.

I'm grateful to reviewers of this thesis, Doc. Sami Romakkaniemi and Dr. Peter Tunved, who provided me valuable comments and suggestions which have improved this thesis considerably.

The financial support from the Vilho, Yrjö and Kalle Väisälä Foundation, Academy of Finland and European Commission is gratefully acknowledged.

I would like to thank all of the co-authors in my articles as well as my colleagues from various institutes; you have made this work not only possible, but also enjoyable. I am especially grateful for Doc. Hannele Korhonen and Doc. Laakso for their considerable efforts to Ion-UHMA model which has been an essential part of this work. I would also like to acknowledge Doc. Tatu Anttila, Doc. Ilona Riipinen, Dr. Stéphanie Gagné, Dr. Hanna Manninen, Dr. Henri Vuollekoski, Dr. Eija Asmi, Dr. Katrianne Lehtipalo, Tuomo Nieminen and Taina Yli-Juuti for scientific collaboration.

Special thanks must be given to my family for always supporting me regardless of the path I have chosen to follow in my life. I would also like to thank my friends for providing me a healthy break from work whenever it was needed and generally making my life more enjoyable. Most of all, I appreciate all the love and support from my wife Virpi, though these written words are not enough to express my gratitude.

Dynamics of neutral and charged aerosol particles

Johannes Markus Leppä
University of Helsinki, 2012

Abstract

Atmospheric aerosol particles have two major effects on everyday life: firstly, they have various climate effects and, secondly, they have adverse health effects. The particles affect climate directly by scattering and absorbing solar radiation and indirectly by acting as cloud condensation nuclei, CCN, with a net effect assumed to be a cooling one. Increase in CCN number concentration may result in brighter and longer lasting clouds, which in turn would increase the amount of radiation scattered back to space. Recent studies suggest that majority of the atmospheric aerosol particles originate from the particle formation occurring via gas-to-particle conversion. However, the freshly-formed particles are not large enough to impact neither health nor climate and they are most susceptible to removal by collisions with larger pre-existing particles. Consequently, the knowledge of both the formation and the growth rate of particles are crucially important when assessing the health and climate effects of atmospheric new particle formation.

The purpose of this thesis is to increase our knowledge of the dynamics of neutral and charged aerosol particles with a specific interest towards the particle growth rate and processes affecting the aerosol charging state. A new model, Ion-UHMA, which simulates the dynamics of neutral and charged particles, was developed for this purpose and it was shown to be capable of reproducing new particle formation and growth events as observed in the measurements. Simple analytical formulae that can be used to estimate the growth rate due to various processes were derived, tested against the simulated data and used to study the effect of charged particles on the growth rate of a particle population. It was found that the average growth rate of freshly-formed particles could be significantly increased due to enhanced condensation onto charged particles. Furthermore, the charged particles were found to increase the growth rate due to self-coagulation and coagulation scavenging by a factor of 1.5–2.

Finally, recent data-analysis methods that have been applied to the aerosol charging states obtained from the measurements were modified for a charge asymmetric framework. The methods were then used on the data measured in Helsinki, Finland, and tested on the data obtained from aerosol dynamics simulations. The methods were found to be able to provide reasonable estimates on the growth rate and proportion of particles formed via ion-induced nucleation, provided that the growth rate is high enough and that the charged particles do not grow much more rapidly than the neutral ones. A simple procedure for estimating whether the methods are suitable for analysing data obtained in specific conditions was provided.

In this thesis, the dynamics of neutral and charged aerosol particles were studied in detail. Combined with the current field and chamber measurements of neutral and charged particles, the analytical tools provided here can be used to study the atmospheric new particle formation and growth more comprehensively and, eventually, to decrease the uncertainty related to climate effects of aerosol particles.

Keywords: atmospheric aerosols, aerosol dynamics, charged particles, modelling of aerosols

Contents

List of publications

This thesis consists of an introductory review, followed by 4 research articles. In the introductory part, these papers are cited according to their roman numerals. **Papers I**, **III** and **IV** are reproduced under the Creative Commons Attribution 3.0 License and **Paper II** is reproduced with the permission granted by the Boreal Environment Research Publishing Board.

I. Leppä, J., Anttila, T., Kerminen, V.-M., Kulmala, M., and Lehtinen, K. E. J.: Atmospheric new particle formation: real and apparent growth of neutral and charged particles, Atmos. Chem. Phys., 11, 4939–4955, 2011.

II. Leppä, J., Kerminen, V.-M., Laakso, L., Korhonen, H., Lehtinen, K. E. J., Gagné, S., Manninen, H. E., Nieminen, T., and Kulmala, M.: Ion-UHMA: a model for simulating the dynamics of neutral and charged aerosol particles, Boreal Env. Res., 14, 559–575, 2009.

III. Gagné, S., Leppä, J., Petäjä, T., McGrath, M. J., Vana, M., Kerminen, V.-M., Laakso, L., and Kulmala, M.: Aerosol charging state at an urban site: new analytical approach and implications for ion-induced nucleation, Atmos. Chem. Phys., 12, 4647–4666, 2012.

IV. Leppä, J., Gagné, S., Laakso, L., Manninen, H. E., Lehtinen, K. E. J., Kulmala, M., and Kerminen, V.-M.: Using measurements of the aerosol charging state in determination of the particle growth rate and the proportion of ion-induced nucleation, Atmos. Chem. Phys. Discuss, 12, 21867–21922, 2012.

1 Introduction

An aerosol is defined as solid or liquid particles suspended in a gas. In the case of atmospheric aerosols, the gas is usually just common air and the word "aerosol" is used loosely as a reference to aerosol particles. The size of the atmospheric particles varies from only a few nanometres up to hundreds of micrometres. Particles of different sizes behave very differently in many ways, so it is useful to divide the particles into subgroups according to their size. In this thesis, the particles are divided into the following size groups according to their diameter: nucleation mode (< 20 nm), Aitken mode (20–100 nm), accumulation mode (0.1–1 μm) and coarse mode (> 1 μm). The particles belonging to the same mode have roughly the same characteristics, though, in some cases, there can be considerable variation even within a mode. The particles with diameter < 1 μm are often referred to as fine particles, though the threshold may vary and a limit of 10 μm is commonly used in legislation.

The main processes affecting aerosol particles in the atmosphere are the new particle formation from gaseous precursors, growth by condensation of vapours onto particle surface, coagulation and, finally, removal of particles by wet and dry deposition, including gravitational settling (Figure 1). The coagulation rate is the highest between a small particle that moves rapidly and a large particle that has a large surface area. As a result, the nucleation and Aitken mode particles need to grow rapidly to larger sizes, or they are removed by coagulation scavenging. The coagulation scavenging is not very efficient for accumulation mode particles and their life time is much longer than that of the smaller ones, thus the name "accumulation mode". The fine particles follow the movement of the air closely, while the coarse particles have more inertia. Thus, the coarse particles are removed more efficiently by gravitational settling than the fine ones.

The origin of particulate matter can be used to divide aerosols into two categories: primary aerosols are emitted into the atmosphere directly as particles and secondary aerosols are formed in the atmosphere via gas-to-particle conversion. Examples of primary sources are sea spray aerosol from oceans (de Leeuw et al., 2011; Jaeglé et al., 2011), dust from deserts (Huneeus et al., 2011), biological particles from vegetation (Després et al., 2012) and soot particles from incomplete combustion (Gaffney and Marley, 2009). Atmospheric nucleation is a secondary source that increases the particle number concentration. Examples of secondary sources increasing the total volume concentration of aerosol particles are condensation of sulphuric acid and low-volatile organic vapours onto particles, aqueous-phase sulphate production in cloud droplets (Goto et al., 2011) or wet aerosols particles (Sievering et al., 1992) and heterogeneous production of secondary organic matter in aerosols or clouds (Zhang and Wexler, 2002; Sorooshian et al., 2010; Lee et al., 2011; Liu et al., 2012). Furthermore, the parti-

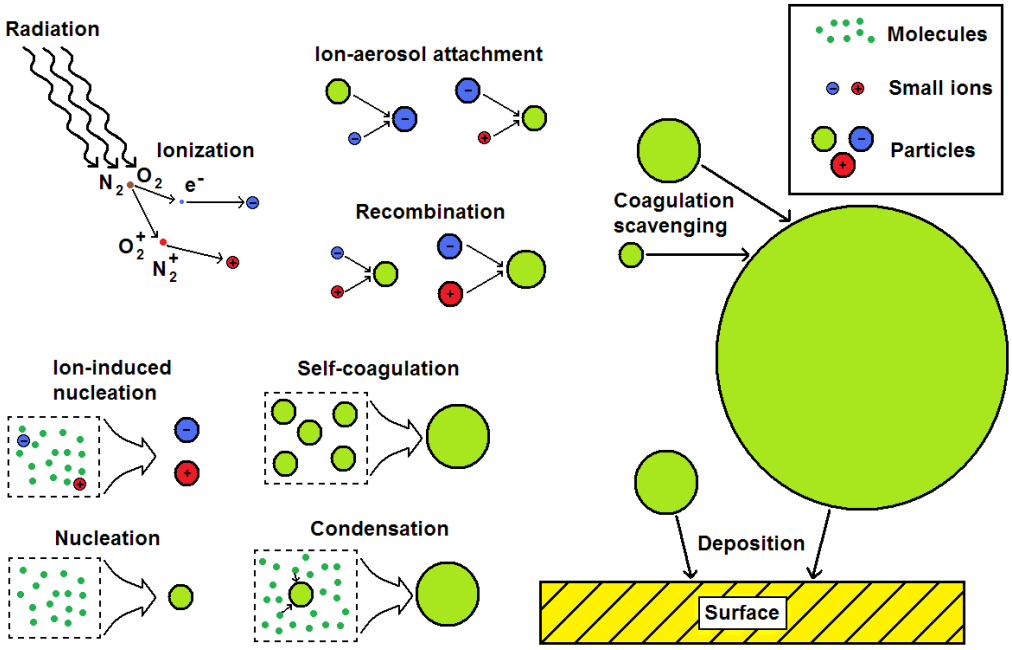

Figure 1. A schematic picture of the processes relevant to this work. Here recombination includes both ion-ion recombination and recombination between oppositely-charged nucleation mode particles, which is also one form of self-coagulation.

cles can originate from biogenic or anthropogenic sources, i.e. from human activities. The composition of the particles depends on their origin, especially with the primary particles, but also on compounds attaching to the particles. Both the size distribution and composition of the particles vary in time and between different locations (Raes et al., 2000; Pöschl, 2005; Jimenez et al., 2009; Asmi et al., 2011).

Atmospheric aerosol particles have various effects on everyday life. Aerosol particles can enter the human body through respiration and cause adverse health effects depending on their composition (Seaton et al., 1995; Anderson, 2009; Gurjar et al., 2010). The size of the particles affects the total deposition efficiency in the respiratory tract and also which region of the tract the particles are most likely to be deposited on (Heyder et al., 1986). Globally, 8 % of lung cancer deaths, 5 % of cardiopulmonary deaths and ~3 % of respiratory infection deaths were associated with fine particulate matter in 2004, with the total number of deaths attributable to urban air pollution being ~1.15 million (WHO, 2004). The susceptibility to adverse health effects associated with the air pollution varies across subpopulations with infants, elderly and people

suffering from respiratory, cardiovascular and other diseases being most at risk (Peled, 2011). In polluted areas, the particles can also significantly reduce the visibility (Hand and Malm, 2007). In the extreme conditions, the aerosol particles can have quite dramatic effects, like disrupting aviation in the case of a volcano eruption (Langmann et al., 2012).

Aerosol particles affect the climate directly by scattering and absorbing the solar radiation and indirectly by affecting the properties of clouds (Seinfeld and Pandis, 1998). The scattering of solar radiation has a cooling effect on the climate, since less radiation reaches Earth's surface, whereas the absorption of the solar radiation results in warming of the climate, since the radiation is captured into the atmosphere. Depending on their composition, aerosol particles with diameter larger than ~30–100 nm may act as cloud condensation nuclei, CCN, and thus affect the cloud properties. The increase in CCN concentration results in an increase of the number concentration of cloud droplets, which in turn may result to a decrease in average size of the droplets, provided that the total volume concentration of water does not change. The increase in droplet concentration may increase the albedo of thin to moderately thick clouds while the albedo of sufficiently thick clouds may be decreased (Twomey, 1977). Furthermore, the increase in droplet concentration may inhibit precipitation and, thus, increase the lifetime of the cloud (Albrecht, 1989). The increased cloudiness and brighter clouds decrease the amount of solar radiation that reaches the Earth's surface and thus cools the climate. The magnitude of the climate effect of aerosols has a large uncertainty (Forster et al., 2007), however, and a lot of effort has lately been put on decreasing these uncertainties (Kulmala et al., 2011).

Recent studies suggest that majority of the atmospheric aerosol particles are formed via gas-to-particle conversion (Spracklen et al., 2006; Kulmala and Kerminen, 2008; Yu et al., 2010; Makkonen et al., 2012). Whether the freshly-formed particles reach the sizes in which they can act as CCN depends on competing processes of growth to larger sizes and coagulation scavenging to larger pre-existing particles (Weber et al., 1997; Kerminen et al., 2001; Kerminen and Kulmala 2002). The growth rate of the nucleation mode particles is of specific interest in this regard, since these particles are most susceptible for coagulation scavenging. A similar competition occurs also between the growth to larger sizes and removal by dry deposition, but the coagulation scavenging is typically much more important removal process for the nucleation and Aitken mode particles than the dry deposition (Kerminen et al., 2004; Pierce and Adams, 2007). The proportion of CCN originating from atmospheric new particle formation is estimated to be up to around 30–70 % (Spracklen et al., 2008; Merikanto et al., 2009).

Observed correlation between the Earth's cloud cover and the magnitude of the flux of galactic cosmic rays, GCR (Svensmark and Friis-Christensen, 1997), has led to studies

exploring the physical connection between the atmospheric ionization and cloudiness, though more recent studies suggest that the correlation may not be robust over long time periods (Agee et al., 2012). One of the physical explanations for this phenomenon is the following: Since GCR is a major source of atmospheric ionization, an increase in GCR results to increased concentration of small ions. The increase in the concentration of small ions may increase the number of particles formed via ion-induced nucleation, IIN, which in turn results in increased number of CCN (Carslaw et al., 2002; Kirkby, 2007). How strongly the cloudiness is modulated by GCR depends, among many other things, on the proportion of IIN of the total formation of secondary aerosol particles. While most of the field measurements indicate that majority of these particles are formed electrically neutral (Laakso et al., 2007a; Gagné et al., 2008, 2010; Manninen et al., 2010), there are also studies suggesting that the new particle formation is dominated by processes involving one or more electric charges (Yu and Turco, 2008; Yu et al., 2010).

This thesis aims to increase our understanding of the role of charged particles and electric interactions with respect to aerosol dynamics. The main goals are to develop an aerosol dynamics model that simulates neutral and charged particles as well as derive equations governing the behaviour of aerosol charging state in conditions in which the concentrations of negative and positive small ions are not the same, i.e. they are asymmetric. As an application of these advances, the methods that have previously been used to analyse aerosol charging state with the assumption of symmetric small ion concentrations (Kerminen et al., 2007; Iida et al., 2008) are developed to cover also conditions in which the small ion concentrations are asymmetric. Furthermore, the applicability of these methods is tested by using them on the data obtained using the newly-developed model. More specifically, the objective of this work has been to answer the following questions:

- What is the role of different processes in the growth of a particle population and how is the growth affected when some of the particles are charged?
- Can we reproduce the time evolution of the charged and neutral particles as observed in the field measurements by using an aerosol dynamics model?
- How does the aerosol charging state behave as a function of particle diameter when the concentrations of the negative and positive small ions are not the same?
- Under which conditions can we determine the growth rate and fraction of particles formed carrying a charge by analysing measured values of the aerosol charging state?

2 Dynamics of neutral and charged particles

2.1 Air ions and electrically charged particles

The atmosphere is constantly ionized through cosmic radiation with the ion-pair production rate varying from ~2 cm^{-3} s^{-1} near the Earth's surface to ~50 cm^{-3} s^{-1} in the stratosphere (e.g. Harrison and Carslaw, 2003; Harrison and Tammet, 2008). Over the land areas, additional ionization is caused by alpha radiation from radon decay and gamma rays emitted from soil and rock with the ion-pair production rates of ~3 and ~4 cm^{-3} s^{-1}, respectively. Furthermore, there are local sources of ionization, like power lines (Eisele, 1989), but their contribution to total ionization of the atmosphere is small.

The radiation typically ionizes an oxygen or a nitrogen molecule, since they are the most abundant molecules in the air. After a chain of chemical interactions, the negative and positive charges are transferred to compounds with the highest and the lowest proton affinities, respectively, depending on the available trace gases (e.g. Harrison and Tammet, 2008). During measurements conducted in a boreal forest, the negative small ions were observed to be dominated by sulphuric acid and its clusters, whereas most distinct peaks observed in the positive mass spectra were associated with n-alkyl pyridines and quinolines (Ehn et al., 2010a).

The concentration of small ions depends on the ionization rate and the sink of ions. Ions are removed by collisions with surfaces, by attaching to aerosol particles and by recombining with each other. The definitions related to the attachment and recombination processes that are used in this thesis are summarized in the nomenclature. Additional losses of small ions may occur, if a new particle is formed around a small ion which subsequently grows to larger sizes. The balance equation of small ions can then be written as

$$\frac{dN_{\mathrm{C}}^{\pm}}{dt} = Q - R^{\pm} N_{\mathrm{C}}^{\pm} - \alpha N_{\mathrm{C}}^{\pm} N_{\mathrm{C}}^{\mp}, \tag{2.1}$$

where $N_{\mathrm{C}}^{\pm}$, Q, and α are the concentration of small (negative or positive) ions, ion-pair production rate and ion-ion recombination coefficient, respectively. Here $R^{\pm}$ is the net removal rate of small ions due to various processes including ion-aerosol attachment, deposition and growth to larger sizes.

Neutral particles are charged and charged particles are neutralized by ion-aerosol attachment. Neutralization is a more rapid process than charging due to attractive interactions between opposite charges. The collision rate of a neutral particle to a small ion is larger than the corresponding collision rate to a neutral cluster of a similar size because of the mirror-charging effect (Figure 2). For two similarly-charged particles or

ions, the Coulomb force is repulsive. Now, when two similarly-charged particles are moving towards each other, the repulsive force slows down the particles and at some point the particles start to move apart. However, if the sum of the radii of the particles is greater than the stopping distance, then the particles can merge to form a particle that has the combined charge of the original particles. With this procedure, large enough particles can get multiply-charged. In atmospheric conditions, it is safe to assume that nucleation mode particles (d_p < 20 nm) are singly-charged (Hoppel and Frick, 1986).

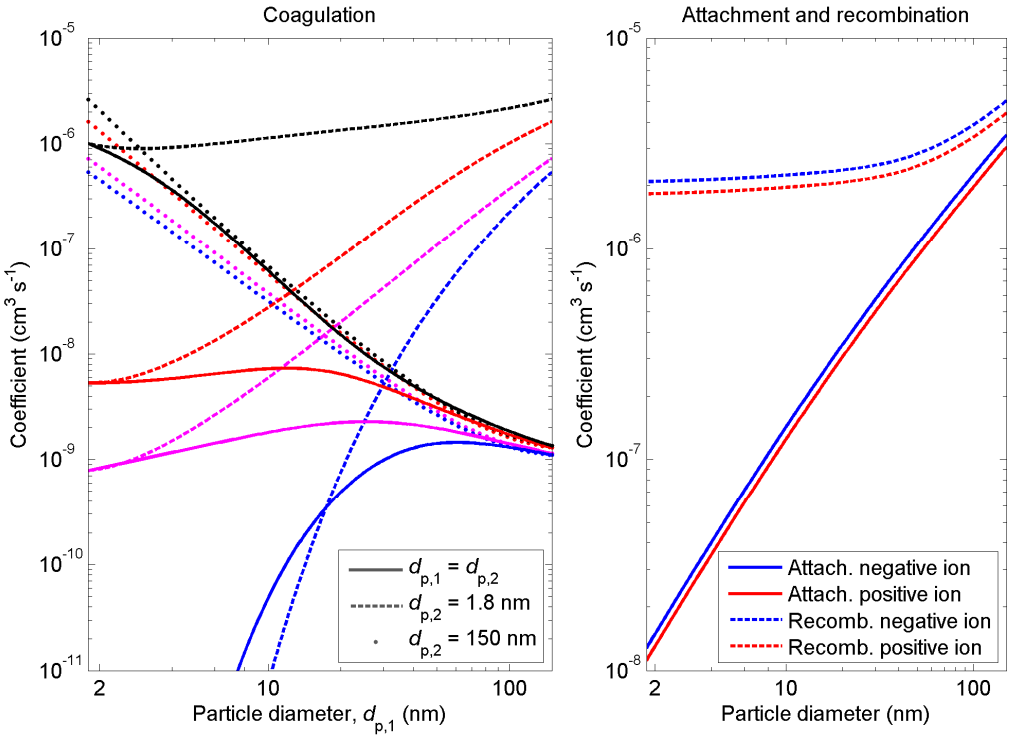

Figure 2. Left panel: Coagulation coefficients as a function of the diameter of one of the coagulating particles, $d_{p,1}$. The diameter of the other particle, $d_{p,2}$, is 1.8 nm, 150 nm or the same as $d_{p,1}$, which is denoted by dashed line, dots or solid line, respectively. The colours indicate whether the coagulating particles are similarly-charged (blue), both neutral (magenta), one charged and the other neutral (red) or oppositely-charged (black). Right panel: Attachment and recombination coefficients of small ions to neutral and oppositely-charged particles, respectively. The difference between the coefficients corresponding to negative and positive small ions, denoted by blue and red lines, respectively, is caused by the different mobilities of the negative and positive small ions.

According to various field measurements, the concentrations of negative and positive small ions can differ by up to a factor of two (Hirsikko et al., 2011). Most ion sources produce the same amount of negative and positive ions, so the difference in concentrations is most probably caused by differences in the sinks of negative and positive ions. In some of the measurements, the average mobility of negative small ions has been observed to be larger than that of positive ones, which is due to the negative ions being smaller than the positive ones. The size difference, in turn, is due to different compositions of negative and positive small ions. A higher mobility results in a higher collision rate to larger particles and surfaces, which in turn results in smaller concentrations. This can be demonstrated by writing Eq. (2.1) in a steady state ($dN_C^{\pm}/dt = 0$) separately for negative and positive small ions and assuming that $R^{\pm}$ consists only of ion-aerosol attachment:

$$0 = Q - \beta_{\mathrm{eff}}^{-} N_{\mathrm{tot}} N_{\mathrm{C}}^{-} - \alpha N_{\mathrm{C}}^{-} N_{\mathrm{C}}^{+} \tag{2.2}$$

and

$$0 = Q - \beta_{\mathrm{eff}}^{+} N_{\mathrm{tot}} N_{\mathrm{C}}^{+} - \alpha N_{\mathrm{C}}^{-} N_{\mathrm{C}}^{+} . \tag{2.3}$$

Here N_{tot} is the total particle concentration and $\beta_{\mathrm{eff}}^{\pm}$ is the effective ion-aerosol attachment coefficient for polydisperse aerosol particles. Let us assume that the attachment coefficient, $\beta_{\mathrm{eff}}^{\pm}$, is linearly dependent on the electrical mobility of the small ion, $Z^{\pm}$, but it is independent of other properties of the ion (Fuchs, 1964; Hõrrak et al., 1998, 2008). Consequently, by combining Eqs. (2.2) and (2.3), we get $Z^{-}N_{\mathrm{C}}^{-} = Z^{+}N_{\mathrm{C}}^{+}$, in other words, if the mobility of negative small ions is larger than that of the positive ones, then the concentration of negative small ions will be smaller than that of positive ones. Other possible sources of imbalance between the negative and positive small ion concentrations are, for example, the transfer of ions by atmospheric electric field (Israël, 1970) and electric mechanism of dry deposition, (Tammet et al., 2001). The latter process results in an imbalance between the ion concentrations, since the electric deposition increases the removal of ions of only one polarity.

2.2 Formation of secondary particles in the atmosphere

Freshly-formed particles consist of multiple molecules and have a diameter of approximately 1–2 nm (Kulmala et al., 2007; Zhang et al., 2012). According to classical nucleation theory there is a threshold diameter that defines the size of the freshly-formed particle (Seinfeld and Pandis, 1998). Clusters smaller than the threshold will more probably shrink through evaporation rather than grow through condensation whereas the opposite holds for particles larger than the threshold size. In homogeneous nucleation particles are formed directly by molecules colliding with each other and

sticking together. In heterogeneous nucleation the particle forms on a pre-existing surface or around a pre-existing core, which can be for example a large molecule or a cluster of molecules. The heterogeneous nucleation is energetically favourable over the homogeneous one, as the energy needed to produce the surface of the particle is smaller (e.g. Seinfeld and Pandis, 1998).

Sulphuric acid has been recognized as one of the key compounds in atmospheric new particle formation (Weber et al., 1996; Sihto et al., 2006; Riipinen et al., 2007; Kuang et al., 2008; Sipilä et al., 2010; Kerminen et al., 2010). However, the binary nucleation of sulphuric acid and water is not able to explain the nucleation observed in the lower troposphere and an additional stabilizing agent is needed (e.g. Weber et al., 2001). Two mechanisms suggested to occur via more stable clusters are ion-induced nucleation, IIN, (e.g. Lovejoy et al., 2004) and ternary sulphuric acid-water-ammonia nucleation (e.g. Korhonen et al., 1999). Recently, it has been observed that amines are much more effective than ammonia in enhancing both neutral and ion-induced sulphuric acid-water nucleation in the atmosphere (Kurtén et al., 2008; Loukonen et al., 2010; Ortega et al., 2012; Paasonen et al., 2012). A stable cluster may also act as a pre-nucleation embryo around which a new particle is formed in heterogeneous nucleation (Hoppel et al., 1994; Kulmala et al., 2004b; Kulmala et al., 2006). In laboratory conditions, a lower supersaturation was observed to be needed for heterogeneous nucleation of charged particles than for that of neutral ones (Winkler et al., 2008).

For particle formation involving more than one compound, it is possible for a certain cluster to be sub-critical for one compound, but being able to grow via another compound (e.g. Seinfeld and Pandis, 1998). In the case of the two-component system, for example, the particle may grow via one compound to a size that is super-critical for the other. In other words, the energy barrier is not surpassed, but rather gotten around. Furthermore, the new particle formation does not necessarily occur via a nucleation process, in which an energy barrier has to be surpassed. Instead, the formation can occur without an energy barrier, in which case the cluster grows by a kinetic rate (McMurry and Friedlander, 1979).

Various new particle formation processes can be divided into two categories: the neutral ones and those involving one or more electric charges. In this thesis, the latter is referred to as ion-induced nucleation (IIN), regardless of whether the formation has occurred via nucleation or some other process. This should not be mixed with ion-mediated nucleation, which in principle includes the ion-induced nucleation and formation of neutral particles through recombination of oppositely-charged small ions (Arnold, 1980).

2.3 Growth of aerosol particles

2.3.1 Definition of growth

The principle of growth is simple: if we have a quantity that somehow describes the size of a particular system, then increase in that quantity describes the growth of that system. However, the practice is not always as straightforward in aerosol physics, as discussed in **Paper I** of this thesis.

In the case of a single particle, the particle diameter is often used to describe the size of the particle. The problem in this approach is that the particles, especially very small ones, are usually not spherical, in which case the geometric diameter is ambiguous. The diameter can be defined according to mass or mobility of the particle, but these diameters are different to each other, especially in nanometre-sizes (de la Mora et al., 2005; Ehn et al., 2011; Larriba et al., 2011). In this thesis, the aerosol particles are assumed to be spherical and thus their geometric diameter is well defined. By growth of a single particle we mean the increase of the diameter of that particle. The particle diameter increases due to condensation of vapour molecules onto the particle surface, which is the only process participating in the growth of a single particle in this approach. The condensational growth proceeds in steps as the molecules are added one by one, but for large enough particles this can be considered as a continuous process occurring at the rate of the average molecular flux.

In the case of a particle population, we need to define the population and to specify the diameter that we use to describe the size of the particles in the population. The rate by which the population shifts to larger sizes is then described by the increase in that diameter. A typical approach is to assume that the particle number size distribution has an approximately log-normal shape and use the geometric mean of the mode to describe the size of the particles in the population (Seinfeld and Pandis, 1998). However, the particle population does not necessarily have a log-normal shape, especially if the population is freshly-formed and has not yet had time to obtain the log-normal shape. In such cases, it is more meaningful to define the diameter in a way that it is not related to the shape of the number size distribution. In this thesis, the count mean diameter is used (**Paper I**). For a discrete representation of a particle size distribution, the count mean diameter, $d_p^\dagger$, is defined as

$$d_p^\dagger = \frac{\sum_{i=1}^{n} N_{tot}^i d_p^i}{\sum_{i=1}^{n} N_{tot}^i}, \tag{2.4}$$

where $d_p{}^i$ and $N_{tot}{}^i$ are the diameter and number concentration of particles in section i, and the particle population is assumed to be covered by sections from 1 to n.

All the particles in a population grow due to condensation, but the condensational growth rate, GR_{cond}, is typically not the same for all of the particles. Nevertheless, a single value of GR_{cond} can be assigned for the population as an increase rate of the diameter describing that population. The average size of the particles in a population increases also due to the coagulation processes. In self-coagulation (i.e. coagulation of particles in the population with each other), the number concentration of the particles decreases, but the average diameter of the particles in the population increases. In coagulation scavenging (i.e. coagulation of particles in the population with pre-existing larger particles), the particles are removed from the population by a diameter dependent rate with the smallest particles most susceptible for removal. In both processes, the diameter used to describe the population increases. However, in the case of the coagulation scavenging, the growth is only apparent, as none of the particles in the population get any larger.

2.3.2 Growth due to condensation

Under most atmospheric conditions, aerosol particles grow mainly due to condensation of vapours onto particle surfaces (Kerminen and Wexler, 1995; Kulmala et al., 2004b). Depending on the size of the particle, the analytical approach to the condensation process varies (Seinfeld and Pandis, 1998). In the free molecular or kinetic regime, particles are close to the size of the condensing molecules and they travel a relatively long distance between consecutive collisions to vapour molecules. In the continuum regime, the particles are multiple orders of magnitudes larger than the surrounding molecules and collisions between the particles and molecules occur constantly. In other words, the particles see their environment as a continuum, rather than separate collisions. Between the kinetic and continuum regime there is a transition regime, in which the analytical approaches to the two other regimes have to be matched. In this section, the condensation is considered in the case of a single component system.

In the kinetic regime, the molecular flux onto a particle of diameter d_p is traditionally given as (e.g. Seinfeld and Pandis 1998):

$$J_{k1} = \frac{\pi}{4} d_p^2 \nu_v \gamma (c_\infty - c_s), \tag{2.5}$$

where subscript "p" and "v" refer to particle and vapour molecule, respectively, ν is the mean thermal speed, c_∞ and c_s are the number concentration of condensing molecules far away from the particle and the saturation vapour concentration at the particle surface, respectively, and γ is the molecular accommodation coefficient. The time derivative of the particle volume is then $dV_p/dt = J_{k1} V_m$, where V_m is the volume of the

condensing vapour molecule. The growth rate of a particle diameter due to condensation is then

$$\mathrm{GR}_{\mathrm{cond,\,k1}} = \frac{1}{2} V_{\mathrm{m}} \nu_{\mathrm{v}} \gamma \left(c_{\infty} - c_{\mathrm{s}} \right). \tag{2.6}$$

In these conditions the growth rate depends on the particle diameter only through the Kelvin effect, which affects the value of c_{s}. The Kelvin effect is caused by the curvature of the surface of a spherical particle and the principle of this phenomenon is the following. The molecules are bound to a liquid phase via interactions with surrounding molecules. Now, as the curvature of the surface increases, the number of surrounding molecules decreases for molecules at the surface and, consequently, the binding energy of the molecules at the surface decreases. In other words, the molecules at the surface of a small particle evaporate more easily than those on the surface of a large particle and a higher supersaturation is needed for the small particle to grow. The Kelvin effect is described quantitatively by the Kelvin equation, which for the saturation concentration can be written as (Seinfeld and Pandis, 1998)

$$c_{\mathrm{s}} = c_{\mathrm{s}}^{0} \exp\left(\frac{4 \sigma V_{\mathrm{m,l}}}{k T d_{\mathrm{p}}} \right). \tag{2.7}$$

Here c_{s}^{0}, $V_{\mathrm{m,l}}$, k, T and σ are the saturation concentration over a flat surface, volume of the condensing molecule in the liquid phase, Boltzmann constant, temperature and surface tension of the condensing compound, respectively. For a non-volatile vapour, c_{s} is negligible, and the growth rate is constant as a function of diameter.

Equations (2.5) and (2.6) hold in the kinetic regime when assuming that the size of the molecule is negligible compared to that of the particle and that the thermal speed of the particle is negligible compared to that of the molecule. The precision of these assumptions decreases with decreasing particle size and a correction is needed for particles smaller than ~10 nm. The corrected flux can be written as (Lehtinen and Kulmala, 2003; Nieminen et al., 2010)

$$J_{\mathrm{k2}} = \frac{\pi}{4} \left(d_{\mathrm{p}}^{2} + d_{\mathrm{v}}^{2} \right) \sqrt{\nu_{\mathrm{p}}^{2} + \nu_{\mathrm{v}}^{2}} \gamma \left(c_{\infty} - c_{\mathrm{s}} \right) \tag{2.8}$$

and the growth rate due to condensation with the corrected flux is then

$$\mathrm{GR}_{\mathrm{cond,\,k2}} = \frac{1}{2} V_{\mathrm{m}} \left(1 + \left(\frac{d_{\mathrm{v}}}{d_{\mathrm{p}}} \right)^2 \right) \sqrt{\nu_{\mathrm{p}}^2 + \nu_{\mathrm{v}}^2}\, \gamma \left(c_\infty - c_{\mathrm{s}} \right). \tag{2.9}$$

As a result, in the case of a non-volatile vapour, the growth rate decreases as a function of diameter until it approaches a constant value when the ratio d_v/d_p approaches zero.

The diameter range of the approximately constant growth rate described above is quite narrow, since the continuum effects start to be important already in sizes below 100 nm. The continuum effects can be taken into account by using a correction factor η, in which case the flux, J_t, can be written as (Nieminen et al., 2010)

$$J_{\mathrm{t}} = \eta J_{\mathrm{k2}} = \frac{8 \left(D_{\mathrm{p}} + D_{\mathrm{v}} \right) \chi}{\left(d_{\mathrm{p}} + d_{\mathrm{v}} \right) \sqrt{\nu_{\mathrm{p}}^2 + \nu_{\mathrm{v}}^2}} J_{\mathrm{k2}}, \tag{2.10}$$

where D is the diffusivity in the air. Here χ is the Fuchs-Sutugin transition regime correction factor (Fuchs and Sutugin, 1971)

$$\chi = \frac{1 + \mathrm{Kn}}{1 + \left(\frac{4}{3\gamma_{\mathrm{m}}} + 0.337 \right) \mathrm{Kn} + \frac{4}{3\gamma_{\mathrm{m}}} \mathrm{Kn}^2}, \tag{2.11}$$

where γ_m is the mass accommodation coefficient and Kn is the Knudsen number. Here J_t is actually a generalized flux that describes not only the transition regime, but particles of all sizes. For the very large particles, the flux given by Eq. (2.10) approaches the flux in the continuum regime (e.g. Seinfeld and Pandis, 1998)

$$J_{\mathrm{c}} = 2\pi \left(d_{\mathrm{p}} + d_{\mathrm{v}} \right) \left(D_{\mathrm{p}} + D_{\mathrm{v}} \right) \left(c_\infty - c_{\mathrm{s}} \right). \tag{2.12}$$

In the continuum regime, the growth rate calculated from the molar flux is the following:

$$\mathrm{GR}_{\mathrm{cond,\,c}} = 4 V_{\mathrm{m}} \frac{d_{\mathrm{p}} + d_{\mathrm{v}}}{d_{\mathrm{p}}^2} \left(D_{\mathrm{p}} + D_{\mathrm{v}} \right) \left(c_\infty - c_{\mathrm{s}} \right) \approx 4 V_{\mathrm{m}} \frac{1}{d_{\mathrm{p}}} D_{\mathrm{v}} \left(c_\infty - c_{\mathrm{s}} \right). \tag{2.13}$$

It then follows that, in the continuum regime, the growth rate decreases linearly as a function of particle diameter.

The growth rates of particles smaller than 20 nm in diameter analyzed from the ambient measurements typically show an increase in the condensational growth rate as

a function of particle diameter (e.g., Hirsikko et al., 2005; Manninen et al., 2010; Yli-Juuti et al., 2011; Kuang et al., 2012). Such behaviour would not be expected, if the growth would be caused mainly by sulphuric acid, in which case the growth rate should occur according to Eq. (2.9). Sulphuric acid has been strongly correlated with the formation of secondary particles (see Section 2.2), but the growth due to condensation of sulphuric acid can explain only about a tenth of the observed growth under majority of atmospheric conditions (e.g. Kuang et al., 2012). One possible explanation for the observed increase in the growth rate as a function of particle diameter is that additional low-volatile vapours begin contributing to the growth as the particles get larger. Thus, the observed growth rate is not caused by any single compound, but it is a sum of multiple compounds, which start to condense onto the particle at different diameters. Alternatively, more volatile organic compounds may participate in chemical reactions in the particle phase, which could restrict the evaporation of those compounds (Monge et al., 2012; Riipinen et al., 2012). Lately, the role of organics in the growth of secondary aerosol particles has been studied extensively (Yu, 2011; Riipinen et al., 2011; Pierce et al., 2011; Donahue et al., 2011) and it is likely that the observed growth is dominated by the organic species.

The growth rates due to condensation and coagulation processes in an example simulation conducted using the Ion-UHMA model are shown in Figure 3. The condensing vapours in this simulation were sulphuric acid, a non-volatile organic vapour and a low-volatile organic vapour. In this case, the condensational growth is mainly due to organic vapours with only a small amount due to sulphuric acid. Also, the non-volatile organic vapour is able to condense onto the smallest particles, but the low-volatile one condenses only to particles larger than ~3 nm in diameter. As a consequence, the total growth rate due to condensation mainly increases as a function of particle diameter up to the size of ~5 nm. In the sizes > ~5 nm in diameter, the value of GR_{cond} decreases, because the vapour concentrations were decreasing during that time. This behaviour demonstrates the problem of separating the time and diameter dependencies of the growth rate when analysing the growth rate from the evolution of a particle number size distribution over a considerable time period.

Condensation of polar molecules may lead to increased condensational flux onto charged particles due to the Coulomb force (Nadykto and Yu, 2003; Lushnikov and Kulmala, 2004). A polar molecule can be described as a compound having a negative and a positive charge set apart by a fixed distance. Now, when a polar molecule arrives to the electric field of a charged particle, it will rotate until it is parallel to the field lines. In this orientation, the end of the molecule that has the same charge as the particle is further away from the particle than the end that has the charge opposite to that of the particle. As the Coulomb force between two charges is inversely

proportional to the square of the distance between the charges, the repulsion between the particle and the similarly-charged end of the molecule is weaker than the attraction between the particle and the oppositely-charged end of the molecule. Thus, as a net effect, a charged particle attracts polar molecules and the strength of the attraction depends on the polarity of the molecule and number of charges on the particle.

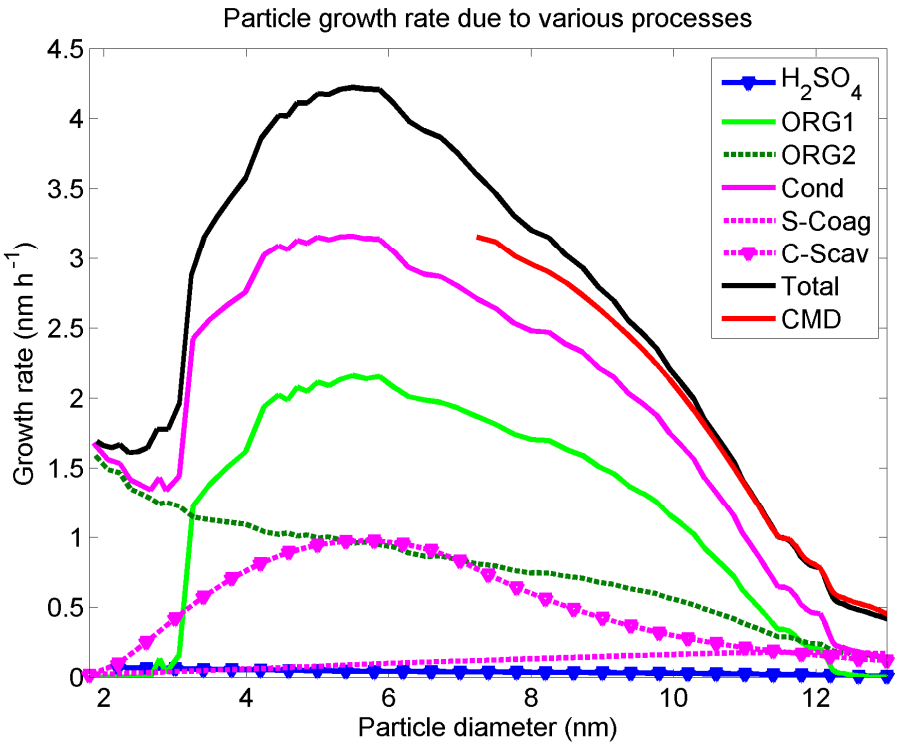

Figure 3. An example of particle diameter growth rates due to various processes as a function of the diameter of the centre of the nucleation mode. The total growth rate due to condensation, "Cond", is a sum of the growth rates due to condensation of sulphuric acid, "H_2SO_4", a low-volatile organic compound, "ORG1", and a non-volatile organic compound, "ORG2". The total growth rate, "Total", is a sum of the growth rates due to condensation, self-coagulation, "S-Coag", and coagulation scavenging, "C-Scav". The growth rate calculated from the change rate of the count mean diameter, "CMD", begins from the diameter of the centre of the nucleation mode at the moment the new particle formation ends.

In this thesis, two different enhancement factors have been used to take the effect described above into account (Figure 4). In **Papers I**, **II** and **IV** we have used the enhancement factor according to Lushnikov and Kulmala (2004):

$$\xi_{\mathrm{LK}}\left(d_{\mathrm{p}}\right)=1+\frac{1}{4\pi\varepsilon_0}\frac{4e^2 r}{kT\left(d_{\mathrm{p}}\right)^2}, \tag{2.14}$$

where e is the elementary charge (1.60×10^{-19} C), d_{p} is the particle diameter in meters, ε_0 is the vacuum permittivity (8.85×10^{-12} F m^{-1}), T is the temperature in Kelvin and k is the Boltzmann constant (1.38×10^{-23} J K^{-1}). Here r denotes the fixed distance between the charges in a polar molecule. The value of r should be chosen according to the condensing compound and the value of 0.125 nm was used in this thesis. In **Paper IV**, we used also the enhancement factor according to Nadykto and Yu (2003):

$$\xi_{\mathrm{NY}}\left(d_{\mathrm{p}}\right)=1+\left(2l_{\mathrm{SA}}E\left(\frac{e^z+e^{-z}}{e^z-e^{-z}}-\frac{1}{z}\right)+a_{\mathrm{SA}}\varepsilon_0 E^2\right)/\left(3kT\right) \tag{2.15}$$

where

$$z=\frac{l_{\mathrm{SA}}E}{kT} \tag{2.16}$$

and

$$E=\left(\frac{1}{\varepsilon_{\mathrm{g}}}-\frac{1}{\varepsilon_{\mathrm{p}}}\right)\times\left(\frac{qe}{4\pi\varepsilon_0\left(0.5\left(d_{\mathrm{SA}}+d_{\mathrm{p}}\right)\right)^2}\right) \tag{2.17}$$

Here l_{SA} is the dipole moment of sulphuric acid (9.47×10^{-30} C m), a_{SA} is the polarizability of sulphuric acid (6.2×10^{-30} m^3), ε_{g} is the relative permittivity of vapour (~1.00 for air), ε_{p} is the relative permittivity of the particle (~100 for bulk sulphuric acid at temperature of 298 K), q is the number of charges in the particle and d_{SA} is the diameter of a sulphuric acid molecule. The distance between the charges in a sulphuric acid molecule can be calculated according to $r_{\mathrm{SA}} = l_{\mathrm{SA}}/e \approx 0.059$ nm, which suggests that the value of r in Eq. (2.14) used in this thesis, 0.125 nm, is rather high. However, the conclusions of this thesis would not change by using a smaller value of r.

The values of the two enhancement factors described above decrease with an increasing particle size (Figure 4). In **Paper I**, it was found that the condensational growth rate of a particle population at sizes < ~5 nm could be considerably higher, if the charged particles grow much more rapidly than the neutral ones, given that a

substantial proportion (≥ 10 %) of the particles are formed via ion-induced nucleation. The magnitude of the increase in the growth rate at a given size depends on the value of the enhancement factor and the fraction of charged particles at a given size. A higher fraction of IIN results in a higher fraction of charged particles at the size in which the particle formation occurs. Furthermore, with smaller concentrations of small ions, the charged particles are neutralized less rapidly and the fraction of charged particles stays higher in the sizes larger than the formation size.

In **Paper IV**, it was shown that if the condensational growth rate of charged particles is higher than that of the neutral ones, the fraction of charged particles will be smaller than in the case of the growth rate being independent of the charge of the particle. This results from the higher loss rate of charged than neutral particles caused by the growth to larger sizes. This phenomenon is important when interpreting measured concentrations and especially so, if only concentrations of charged particles are measured.

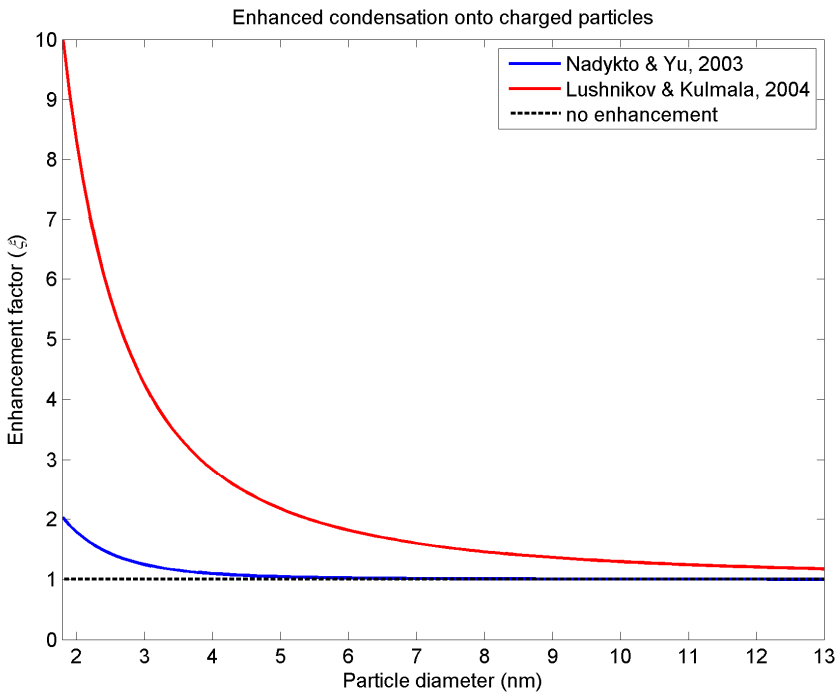

Figure 4. The growth enhancement factors that describe the enhanced condensation onto charged particles compared to that onto the neutral ones. The blue and red lines denote the enhancement factors according to Nadykto and Yu (2003) and according to Lushnikov and Kulmala (2004), respectively, with the dashed line denoting unity (i.e. no enhancement).

2.3.3 Growth due to self-coagulation

Two slightly different processes can be defined as self-coagulation: the coagulation of two particles having the same diameter or the coagulation of two particles belonging to the same particle mode, i.e. intramodal coagulation. In this thesis, the latter definition is used.

The coagulation is defined as collision and coalescence of two particles. From a single particle point of view, two particles are lost and one new particle appears. From a particle population point of view, the particle number concentration decreases, but the average size of the particles increases, since the total volume of the particles does not change. Thus, the diameter used to describe the particle population grows due to self-coagulation.

In **Paper I**, an analytical expression for estimating the growth rate due to self-coagulation was derived with the help of a simplifying assumption that the particle number size distribution of the population can be described by a monodisperse distribution. By assuming further that the particles are neutral or carry a single negative or positive charge, that distribution is fully described by the diameter of the particles, d_p, and number concentrations of neutral, negative and positive particles, N_0, N_- and N_+, respectively. As the relation between the diameter and volume of a spherical particle is trivial, the total volume concentration of the particles is readily calculated from the number concentrations and diameter. Now, the total volume concentration does not change in self-coagulation, in which case the decrease in number concentration results in an increase in the diameter. The growth rate of the particle diameter due to self-coagulation, $\mathrm{GR}_{\mathrm{scoag}}$, can then be written as

$$\begin{aligned}\mathrm{GR}_{\mathrm{scoag}}\left(d_\mathrm{p}\right) = \frac{d_\mathrm{p}}{3N_{\mathrm{tot}}}\Big[0.5\big(k_{0,0}\left(d_\mathrm{p}\right)N_0^2 + k_{-,-}\left(d_\mathrm{p}\right)N_-^2 + k_{+,+}\left(d_\mathrm{p}\right)N_+^2\big) \\ + k_{0,-}\left(d_\mathrm{p}\right)N_0N_- + k_{0,+}\left(d_\mathrm{p}\right)N_0N_+ + k_{-,+}\left(d_\mathrm{p}\right)N_-N_+\Big]\end{aligned}, \tag{2.18}$$

where $k_{\mathrm{q1,q2}}$ is the self-coagulation coefficient between particles with charges q1 and q2 and N_{tot} is the total number concentration of particles. Assuming that all the particles in the population are neutral, Eq. (2.18) simplifies to

$$\mathrm{GR}_{\mathrm{scoag}}\left(d_\mathrm{p}\right) = \frac{d_\mathrm{p}}{6}k_{0,0}\left(d_\mathrm{p}\right)N_{\mathrm{tot}}\,. \tag{2.19}$$

Equations (2.18) and (2.19) are exact only for a monodisperse distribution. However, they can be used to estimate the growth rate due to self-coagulation even if the

population consists of particles with varying sizes, but the accuracy of the estimation decrease as the width of the size range of the particles increases.

The value of GR_{scoag} in the example simulation is shown in Figure 3. In this case, GR_{scoag} is not a major component of the total growth rate. The value of GR_{scoag} increases with increasing particle size, which is a net effect of the following three aspects: (1) linear increase of the value of GR_{scoag} as a function of diameter, which is explicitly written in Eqs. (2.18) and (2.19), (2) simultaneous decrease in the value of N_{tot} and the growth to larger sizes and (3) changes in the self-coagulation coefficients as a function of diameter (Figure 2).

In **Paper I**, it was shown that Eqs. (2.18) and (2.19) can be used to determine the growth rate due to self-coagulation of a nucleation mode in atmospherically relevant conditions. Also, when charged particles were included in a simulation, the growth rate due to self-coagulation was observed to increase on average by a factor of ~2 when compared to corresponding simulations with only neutral particles. This is caused by the larger values of coagulation coefficients when one of the coagulating particles is charged or both particles are oppositely-charged compared to corresponding values in the case of two neutral particles coagulating (Figure 2).

2.3.4 Growth due to coagulation scavenging

In the atmosphere, nucleation and Aitken mode particles are removed by coagulation with pre-existing larger particles, which is denoted as coagulation scavenging. The removal rate of the particles decreases with increasing particle diameter, i.e. the smaller particles are removed more efficiently than the larger ones. As a result, the average diameter of the particles in the mode increases due to coagulation scavenging, but the growth is only apparent, as the particles do not actually get any larger.

Stolzenburg et al. (2005) studied the growth rate due to coagulation scavenging in the case of a growing log-normal mode. However, the shape of a freshly-formed particle mode, for which the coagulation scavenging is most efficient, is typically not log-normal, as the shape depends mainly on the profile of the new particle formation rate as a function of time. In **Paper I**, a theory that applies for distributions of any shape was developed. That theory is based on estimating the change rate of the count mean diameter, $d_p^{\dagger}$, defined in Eq. (2.4), due to coagulation scavenging. Using a discrete representation of the particle number size distribution, the growth rate due to coagulation scavenging is given by

$$\mathrm{GR}_{\mathrm{scav}} = d_{\mathrm{p}}^{\dagger} \frac{\sum_{i=1}^{n} \mathrm{CoagS}^{i} N_{\mathrm{tot}}^{i}}{\sum_{i=1}^{n} N_{\mathrm{tot}}^{i}} - \frac{\sum_{i=1}^{n} \mathrm{CoagS}^{i} N_{\mathrm{tot}}^{i} d_{\mathrm{p}}^{i}}{\sum_{i=1}^{n} N_{\mathrm{tot}}^{i}} \quad , \tag{2.20}$$
$$= d_{\mathrm{p}}^{\dagger} \times \mathrm{CoagS}^{\dagger} - \left(d_{\mathrm{p}} \times \mathrm{CoagS}\right)^{\dagger}$$

where $N_{\mathrm{tot}}{}^{i}$ and CoagS^{i} are the particle number concentration and coagulation sink of particles in the size section i, and the growing mode is assumed to be covered by size sections from 1 to n. The dagger (†) denotes the count mean value averaged over the growing mode.

When deriving Eq. (2.20), the particle charges were not taken into account. However, the coagulation sink depends on the diameter and charge of the particle, as well as on the distribution of charges in the pre-existing larger particles. The mathematical analysis that resulted in Eq. (2.20) can be performed also when the particles in each size section are divided further into three charge classes, namely neutral, negatively-charged and positively-charged. In this case, the count mean values of the diameter, $d_{\mathrm{p}}^{\ddagger}$, and coagulation sink, $\mathrm{CoagS}^{\ddagger}$, are calculated as an average over the size sections and charge classes using the number concentration in each size section and charge class as the weighting parameter:

$$d_{\mathrm{p}}^{\ddagger} = \frac{\sum_{i=1}^{n} \left(N_{0}^{i} + N_{-}^{i} + N_{+}^{i}\right) d_{\mathrm{p}}^{i}}{\sum_{i=1}^{n} \left(N_{0}^{i} + N_{-}^{i} + N_{+}^{i}\right)} \tag{2.21}$$

$$\mathrm{CoagS}^{\ddagger} = \frac{\sum_{i=1}^{n} \left(\mathrm{CoagS}_{0}^{i} N_{0}^{i} + \mathrm{CoagS}_{-}^{i} N_{-}^{i} + \mathrm{CoagS}_{+}^{i} N_{+}^{i}\right)}{\sum_{i=1}^{n} \left(N_{0}^{i} + N_{-}^{i} + N_{+}^{i}\right)} . \tag{2.22}$$

Here the lower and upper indices denote the charge class and size section, respectively, and the distribution of charges in the pre-existing larger particles are taken into account when estimating the values of $\mathrm{CoagS}_{q}{}^{i}$. With these definitions, the growth rate due to coagulation scavenging is given by

$$\mathrm{GR}_{\mathrm{scav}} = d_{\mathrm{p}}^{\ddagger} \times \mathrm{CoagS}^{\ddagger} - \left(d_{\mathrm{p}} \times \mathrm{CoagS}\right)^{\ddagger} . \tag{2.23}$$

The difference between Eqs. (2.20) and (2.23) is that the count mean value in Eq. (2.20) is calculated over the size sections, whereas the count mean value in Eq. (2.23) is calculated over the size sections and charge classes. The number of charge classes was limited to three in this analysis, which is not a good assumption in the case of the pre-existing larger particles (Hoppel and Frick, 1986). However, the additional charge

classes for the pre-existing larger particles would have only a minor effect on the values of the coagulation sink for the following reasons: In the case of the coagulation sink of the charged particles, both the attraction between oppositely-charged particles and the repulsion between similarly-charged particles would be increased, but these two phenomena would mostly cancel each other out. In the case of the neutral particles, the coagulation sink would be increased due to the mirror-charge effect, but that effect is not particularly strong (Figure 2).

In **Paper I**, it was shown that the apparent growth rate of a nucleation mode due to coagulation scavenging was a factor of ~1.7 higher, on average, when charged particles were included in the simulation than in the case of purely neutral simulation. However, the magnitude of the growth rate due to coagulation scavenging was found to be very dependent on the shape of the nucleation mode and on the average diameter of the particles. A wider mode resulted in a higher growth rate. The effect of the particle size was a bit more complicated, but the value of the growth rate due to coagulation scavenging was typically highest when the average diameter of the mode was ~5 nm. When the average diameter was much smaller than 5 nm, the mode was too narrow to grow effectively by the coagulation scavenging. When the average diameter was much larger than 5 nm, the relative difference in the particle sizes within the mode was not large enough for the growth due to coagulation scavenging to be effective. This phenomenon is observed also in the case of the example simulation shown in Figure 3.

3 Aerosol dynamics model Ion-UHMA

Most of the work in this thesis is based on simulations of dynamics of neutral and charged aerosol particles. For this purpose, a new model called Ion-UHMA (University of Helsinki Multicomponent Aerosol model for neutral and charged particles) was developed (**Paper II**). The model builds on the aerosol dynamics models UHMA (Korhonen et al., 2004) and AEROION (Laakso et al., 2002). The Ion-UHMA solves the time evolution of particle number and volume size distributions by simulating the dynamics of neutral and electrically charged aerosol particles in atmospheric conditions.

3.1 Size and charge distribution description

Ion-UHMA is a sectional box model. The upper and lower limits of the simulated particle diameter range are specified by the user, but it is recommended to exclude particles smaller than ~1.5 nm or larger than ~1000 nm, since the parameterizations employed in the model might not hold for particles that small or large, respectively. The particles in the model are divided into user specified number of size sections and every size section is divided into three charge classes: neutral, negative and positive. In order to reduce the computational burden, all the particles are at most singly-charged, which is a good assumption for particles smaller than 20 nm in diameter (Hoppel and Frick, 1986).

The sectional method used in Ion-UHMA is the fixed hybrid method (Jacobson and Turco, 1995), in which the particles are divided into sections of fixed size according to the volume of their core compounds. The division is done in a way that conserves the particle number and volume concentrations. The radii of particles are then determined by calculating the amount of noncore compounds, in this case assuming that the particles reach equilibrium with ambient ammonia and water.

Besides the particle distribution described above, the model includes pools for negative and positive small ions. The small ions represent molecular clusters or large molecules that are smaller than the freshly-formed particles and such ions are constantly observed in the measurements of charged particles. The electrical mobilities of the negative and positive small ions used in this thesis were 1.60 and 1.40 $cm^2\ V^{-1}\ s^{-1}$, respectively, which correspond to mobility diameters of ~1.16 and ~1.24 nm, respectively (Ehn et al., 2011). These ions are allowed to attach to neutral and oppositely-charged particles and to recombine with each other. The concentrations of small ions can be calculated dynamically using the ion production rate as an input in the model and simulating the sink of small ions or the small ion concentrations can be used as inputs in the model.

3.2 Particle composition

The particles in the model are divided into the size sections based on the volume of their core. The core compounds constitute of condensing and non-condensing vapours. The condensing vapours are sulphuric acid and a few organic compounds, which represent the variety of organic species present in the atmosphere. The non-condensing compounds describe species like mineral dust and black carbon, which may, for example, exist in the large particles in the beginning of the simulation, but which are not allowed to condense onto or evaporate from the particles. The water and ammonia contents are not included in the core of the particles, but their amount in the particles is calculated assuming that the particles are in equilibrium with ambient ammonia and water (Napari et al., 2002). The chemical composition of particles is traced individually for each size section and charge class, but all the particles with the same size and charge are assumed to have the same composition.

3.3 Aerosol microphysics

The aerosol dynamics processes included in the Ion-UHMA will be described next with the emphasis on the way in which they are incorporated in the model. The principles of the processes can be seen in Figure 1 and the processes were discussed in more detail in Sections 2–2.3.4.

3.3.1 Gas-to-particle conversion

The Ion-UHMA model does not aim to simulate the actual nucleation process. Instead, our approach is to take as model inputs the formation rates of neutral and charged particles at sizes (around 1.5–2 nm) where these particles are ready to grow by vapour condensation. By this way, simulated particles can be thought to be nucleated thermodynamically or kinetically via neutral or ion-induced pathways, and the particle growth may either follow directly the nucleation or the clustering process or start from the "activation" of neutral clusters or small ions (Hoppel et al., 1994; Kulmala et al., 2006). In the simulations conducted in **Papers I**, **II** and **IV**, the diameters of the freshly-formed particles were assumed to be 1.5, 2.0 and 1.8 nm, respectively.

3.3.2 Condensation

Condensation of vapour molecules on the particle surfaces is the most important process behind the observed growth of aerosol particles in the atmosphere. Conventionally, the flux of molecules onto the particle surface is calculated assuming that the diffusion coefficient of the particle is negligible compared to that of vapour molecule and that the size of the vapour molecule is negligible compared to that of the particle. These assumptions become less valid as the particles get smaller and

eventually close to molecular sizes. In the Ion-UHMA, the non-continuum effects in the collision rates are corrected using the formulation by Fuchs and Sutugin (1971), which is furthermore corrected according to Lehtinen and Kulmala (2003) to take into account the molecule-like properties of nanometre-sized particles.

The collision frequency of dipole molecules to charged particles is enhanced due to Coulomb force. In Ion-UHMA, this can be taken into account using the enhancement factor either according to Lushnikov and Kulmala (2004), $\xi_{LK}(d_p)$, or according to Nadykto and Yu (2003), $\xi_{NY}(d_p)$. The values of these enhancement factors are shown in Figure 4. Both of these factors depend strongly on the particle diameter, d_p, and have considerable effect only in nanometre-sizes.

The condensing vapours in Ion-UHMA are sulphuric acid and a few organic compounds that describe the net effect of all organic compounds. Sulphuric acid is known to have very low saturation vapour pressure and in the model it is assumed to be non-volatile. The variety of low- or semi-volatile organic vapours in the atmosphere is huge (Goldstein and Galbally, 2007) and the knowledge of their properties is limited. For the sake of simplicity, the organic vapours in Ion-UHMA are described by only a few compounds. The number and properties of these compounds are set by the user depending on the work at hand. For each compound, the equilibrium vapour pressure over the particle surface is calculated either by using the Kelvin equation or by using the nano-Köhler theory (Anttila et al., 2004; Kulmala et al., 2004a). The former takes into account only the curvature of the particle, while the latter also takes into account the composition of the particle. Now, when estimating the magnitude of the Kelvin effect in the case of a multicomponent system, the surface tension, σ, in Eq. (2.7) is that of the particle and the value of the surface tension depends on the composition of the particle. However, for the sake of simplicity, a single value (σ = 50 mN m^{-1}) is used for all particles in the model.

The condensational growth cannot be simulated exactly with a model that uses fixed sections to describe the particle number size distribution. As an example, when all the particles in a size section grow by the same rate, they reach the same size after one time step. Now, the size that the particles have reached is typically none of the fixed sizes in the model, so the particles are divided into two consecutive size sections closest to the particle size after the time step. As a consequence, the particle population that was initially in one section is now divided into two sections. This artificial broadening of the size distribution is called numerical diffusion (Jacobson, 2005). The simplest way of reducing the effect of numerical diffusion is to increase the number of size sections, but this approach increases the computational burden also. The numerical diffusion not only distorts the shape of the particle number size distribution, but also results in an underestimation of the condensational growth rate of the particle

population (**Paper I**). This underestimation increases with increasing width of the population, i.e. with increasing diameter range covered by the population.

In Ion-UHMA, the division of the particles into consecutive size sections is done in a way that conserves the particle number concentration and the total volume concentration. In **Paper I**, it was shown that this approach underestimates the average diameter of the particles. The effective growth rate in this case can be approximated as (**Paper I**):

$$\mathrm{GR}_{\mathrm{eff}} = \frac{3}{1+\lambda+\lambda^2}\mathrm{GR}_{\mathrm{cond}} \tag{3.1}$$

where λ is the ratio between the diameters corresponding to consecutive size sections ($\lambda = d_{\mathrm{p}}^{i}/d_{\mathrm{p}}^{i+1}$). The value of λ approaches unity with increasing number of size sections. As the effect of numerical diffusion, described above, also decreases with increasing number of size sections, it is important to consider the number of size sections used when simulating condensational growth using fixed sectional approach.

3.3.3 Coagulation

Coagulation includes three processes in the model: collisions between particles, attachment of small ions to particles and recombination of small ions. The coagulation coefficients are calculated using the flux matching theory according to Fuchs (1964). In case of one or both of the particles being charged, the coagulation coefficient is corrected according to Howard et al. (1973) and Mick et al. (1991). This correction takes into account both Coulomb and Van der Waals forces. The attachment coefficient between a small ion and a particle is based on the expression of attachment coefficient by Fuchs (1964) which is corrected according to Hõrrak et al. (1998) to match the tabulated results of Hoppel and Frick (1990) and experimental data by Reischl et al. (1996). The ion-ion recombination coefficient of negative and positive small ions in the model is set equal to 1.6×10^{-6} $\mathrm{cm}^3\ \mathrm{s}^{-1}$ (Nolan, 1941; Hoppel and Frick, 1990; Tammet and Kulmala, 2005). The attachment and coagulation coefficients are illustrated in Figure 2.

3.3.4 Dry deposition

In dry deposition, the particles are removed from the carrier gas by collisions and attachment to surfaces. In Ion-UHMA, the dry deposition is treated using the semi-empirical deposition model according to Rannik et al. (2003). The model is based on flux measurements that were limited to particles with diameter from 10 to 500 nm. In the parameterization implemented to Ion-UHMA, the model is extrapolated to sizes

below 10 nm while accounting for the size dependence of deposition velocity controlled by the Brownian deposition mechanism.

In theory, the dry deposition of charged particles may be enhanced due to electrical interactions. The electric field of the atmosphere is strongly enhanced on the tips of the leaves and needles of the plants, which increases the deposition velocity of the particles of one polarity while the particles of the other polarity are not deposited due to repulsion (Tammet et al., 2001). The magnitude of the electric deposition depends on the strength of the atmospheric electric field. Near the surface of the Earth, the strength of the electric field is typically in the range of 100–200 V m^{-1} in fair weather conditions, but the value may exceed 10 kV m^{-1} in thunderstorm situations (Israël, 1973). In fair weather conditions, a wind speed < 0.2 m s^{-1} is needed for the electric deposition to be as important as the dry deposition due to other processes for particles in the range of 6–300 nm (Tammet et al., 2001). In thunderstorm situations, the electric deposition may be important for somewhat higher wind speeds and for all particles smaller than 1 μm in diameter. The electric deposition is not taken into account in the Ion-UHMA model, in which charged particles are treated the same way as neutral ones when calculating the dry deposition.

3.4 Reproducing a nucleation event as observed in the measurements

An observation of freshly-formed particles and their subsequent growth to larger sizes is called a nucleation event, or shortly just an event (Mäkelä et al., 1997; Dal Maso et al., 2005). Such events have been observed in almost all of the environments in which adequate instruments have been measuring aerosol size distributions, with the Amazonian rainforest being a notable exception (e.g. Martin et al., 2010). The features of a typical event differ between different sites. The events can be divided into local and regional ones depending on whether the new particle formation is assumed to take place over a small restricted area or over a large area, respectively. An example of local events are the coastal events observed at Mace Head, Ireland, in which the new particle formation occurs over a narrow band of algae exposed to the sun during a low tide (O'Dowd et al., 2002). The events observed at the SMEAR II station in Hyytiälä, southern Finland (Hari and Kulmala, 2005), are typically regional ones (Dal Maso et al., 2005). Much of our knowledge on atmospheric new particle formation is based on the analysis of the events observed in various measurements.

In field measurements, the instruments have a fixed location, but the air they measure changes constantly. This means that a difference observed between two consecutive values in a measured time series does not necessarily describe a change in that value within a particle population, but rather a difference in that value between two particle populations. However, when analysing regional events, the conditions surrounding the

measurement site are assumed to be homogeneous over large areas. Thus, the air masses are assumed to spend time in similar conditions over long periods of time and consequently, the changes observed in a measured time series are assumed to represent the actual changes that would be observed by following a specific particle population. This means, for example, that if the average diameter of nucleation mode particles increases between consecutive observations in a time series, this can be assumed to represent the actual growth rate of the nucleation mode particles. These kinds of assumptions cannot be made for the local events (Ehn et al., 2010b).

The Ion-UHMA simulates the time evolution of a particle population as if following the same air parcel all the time. This is not the same as what is measured at the field stations, but the two are comparable in situations in which the homogeneity assumption described above holds. In **Paper II**, a set of events observed at the SMEAR II station were reproduced using the Ion-UHMA. The new particle formation rate, particle diameter growth rates, concentrations of particles with the diameter larger than 20 nm and concentrations of small ions were taken from measurements and used as input in the model. The model was able to reproduce the main features of all of the chosen events and a particularly good correspondence between simulated and measured evolutions of particle number size distributions was observed for the event measured during 15 September 2006 (Figure 5). Probably the best indication of the excellence of this reproduction is the boundary between the simulation and the measurements at 20 nm, at which the two merge almost seamlessly. Another important point is that besides the evolution of total particle population, the Ion-UHMA was also able to reproduce the main features of the evolution of the charged particles.

Being able to reproduce the observed new particle formation events has two important implications. Firstly, the physics the model is based on is sufficiently accurate to simulate the dynamics of both the neutral and the charged particles, which is the foundation of most of the work of this thesis. Secondly, it indicates that the data-analysis methods that have been used to determine the new particle formation rate and the particle growth rate from the measured size distributions are able to provide reasonable estimates. This is not only important from data-analysis point of view, but also demonstrates how the model could be used to test new data-analysis methods.

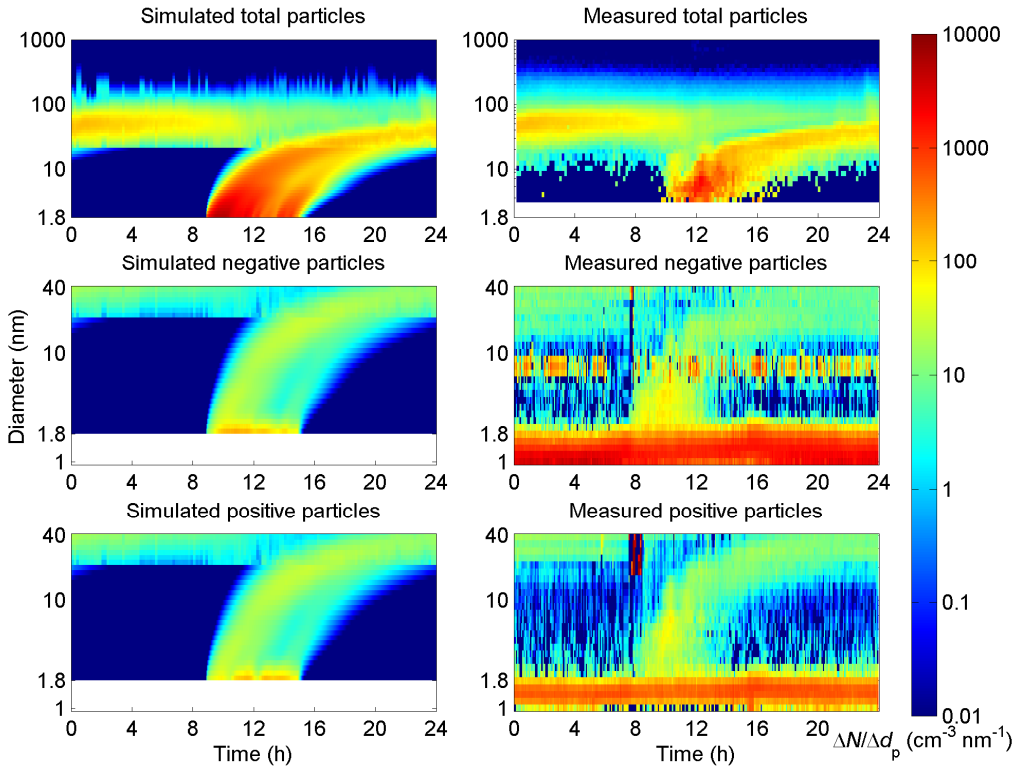

Figure 5. An example of evolution of the particle number size distribution as observed in the field measurements (panels on the right) and a corresponding reproduction made using the Ion-UHMA (panels on the left). The measured size distribution of total particles from 20 to 1000 nm and concentrations of small ions were used as input in the model, as were new particle formation rates and particle growth rates determined from the measured data. The measurements were conducted using differential mobility particle sizer (Aalto et al., 2001) for total particles and air-ion spectrometer (Mirme et al., 2007) for charged particles and small ions.

4 Applications: determination of the growth rate and proportion of ion-induced nucleation from the aerosol charging state

The physical principle governing the distribution of charges as a function of particle diameter was described in Section 2.1 and the fraction of charged particles in steady state conditions can be estimated according to those principles (Hoppel and Frick, 1986). The fraction of charged particles in the steady state depends on the size of the particles and on the specific conditions. However, the actual fraction of charged particles may deviate from the steady state value, especially in the size ranges in which the new particle formation is assumed to occur. If even a few percent of the particles are formed via IIN, the charged fraction will be significantly above the corresponding value in the steady state. Mainly because of ion-aerosol attachment, the initial charged fraction approaches the value in the steady state, and the particles grow to larger sizes simultaneously. Depending on the particle growth rate and the change rate of the charged fraction, the initial deviation from the steady state may partly exist in the sizes in which it can be measured with current instruments. Consequently, the observed behaviour of the charged fraction as a function of particle diameter can be extrapolated to smaller sizes in order to provide information of the proportion of IIN and of the particle growth rate (Kerminen et al., 2007; Iida et al., 2008). Two data-analysis methods, the iteration and the fitting method, and the underlying physics related to this phenomenon are discussed in detail in the next two sections.

4.1 Definition of the charged fraction and iteration method

The charged fraction, $f^{\pm}$, is defined as the ratio of the concentration of charged particles to the total particle concentration, $f^{\pm} = N_{\pm}/N_{\mathrm{tot}}$. In this thesis, the charged fraction at the size of the particle formation is referred to as initial charged fraction and it depends on the proportion of particles formed via IIN. After the formation, the population is subject to ion-aerosol attachment, self-coagulation and coagulation scavenging, all of which are processes that may change the charged fraction. Under most conditions, the most important process changing the charged fraction is the ion-aerosol attachment, which includes charging of neutral particles and neutralization of charged ones. Assuming that the particles do not grow, after some time the neutralization and charging of particles are at balance and the charge fraction does not change any more. This value is called the equilibrium charged fraction and it depends on the size of the particles (Figure 6). If the charged fraction is smaller (larger) than the corresponding value in charge equilibrium, the particle population is said to be undercharged (overcharged).

As the freshly-formed particles grow to larger sizes, both the charged fraction and the equilibrium charged fraction change. Eventually, the charged fraction asymptotically

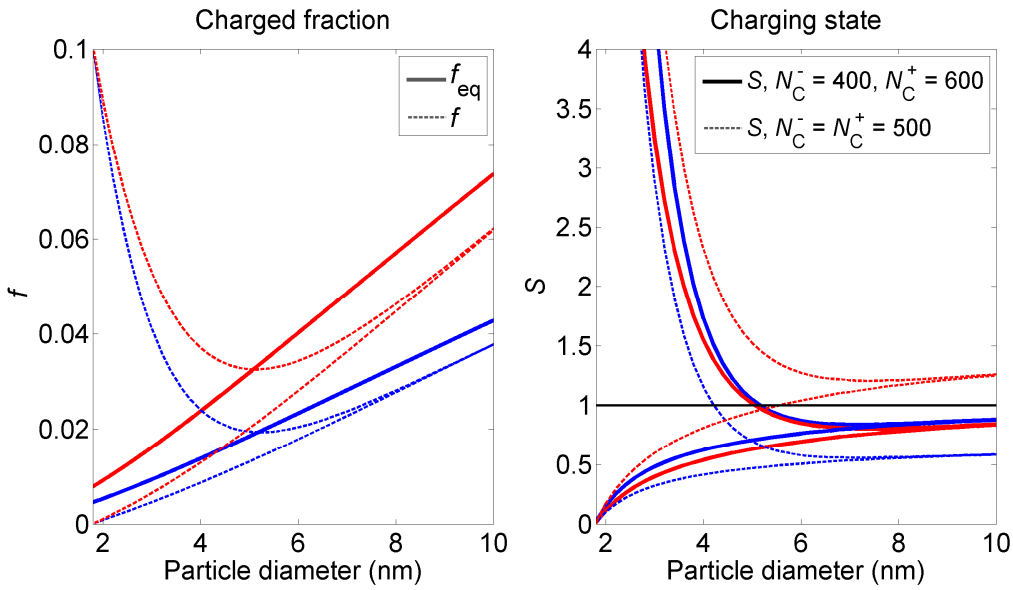

Figure 6. Left panel: Charged fraction as a function of particle diameter. The solid lines denote the equilibrium charged fraction and the dashed lines denote charged fractions starting from 0 or 0.1 at 1.8 nm with the blue and red colours denoting the negative and positive charged fractions, respectively. The concentrations of negative and positive small ions are 400 and 600 cm^{-3}, respectively, and the particle diameter growth rate is 5 nm h^{-1}. Right panel: The behaviour of aerosol charging state as a function of particle diameter corresponding to the charged fractions depicted in the left panel. The solid (dashed) lines denote a case in which the asymmetry in the small ion concentrations has (has not) been taken into account, when estimating the equilibrium charged fraction.

approaches the value in charge equilibrium as shown in Figure 6. There are two points of interest in Figure 6: (1) The merging of the two lines that depict the charged fractions that were initially in over- and undercharged states. (2) The crossing of the lines that depict the equilibrium charged fraction and the charged fraction initially at overcharged state. The former denotes the diameter at which the information of the initial charged fraction has been lost due to changes in the charged fraction. The latter builds up in the following way: The net effect of the processes changing the charged fraction drives the charged fraction towards the equilibrium. The rate of this change depends on the difference of the charged fraction at the given diameter and the corresponding value at the equilibrium. As the charged fraction drops close to the value in equilibrium, the change rate of charged fraction approaches zero, which is achieved

at the point in which the charged fraction reaches the value in equilibrium. However, the particles continue to grow to larger sizes in which the equilibrium value of the charged fraction is also larger. Now, the charged fraction does not reach this new equilibrium value instantaneously and, as a result, the charged fraction ends up in the undercharged state.

The behaviour of charged fraction as a function of diameter depends on the small ion and particle concentrations, particle growth rate and initial fraction of charged particles (Iida et al., 2008; **Papers III** and **IV**). Previously, the charged fractions have been considered in a charge symmetric framework, in which the concentrations of negative and positive ions and those of negative and positive particles are assumed to be the same (Iida et al., 2008). Furthermore, the attachment and the recombination coefficients of negative and positive ions are assumed to be the same and, consequently, the negative and positive charged fractions are the same. In the work of this thesis, the charged fractions have been considered in a charge asymmetric framework, in which the assumptions listed above have not been made (**Papers III** and **IV**). In the asymmetric framework, by neglecting the self-coagulation and the coagulation scavenging, the behaviour of the charged fraction as a function of diameter is the following (**Paper III**):

$$\left(\frac{df^-}{dd_\mathrm{p}}\right) = \mathrm{GR}^{-1}\left(\left(1 - f^- - f^+\right)\beta^- N_\mathrm{C}^- - \alpha^+ f^- N_\mathrm{C}^+\right) \tag{4.1}$$

and

$$\left(\frac{df^+}{dd_\mathrm{p}}\right) = \mathrm{GR}^{-1}\left(\left(1 - f^- - f^+\right)\beta^+ N_\mathrm{C}^+ - \alpha^- f^+ N_\mathrm{C}^-\right). \tag{4.2}$$

Here β^q is the attachment coefficient of a small ion with charge q to a neutral particle, α^q is the recombination coefficient of a small ion to oppositely-charged particle and GR is the condensational growth rate, which is assumed to be the same for neutral and charged particles. Equations (4.1) and (4.2) have to be solved simultaneously, since the behaviour of the negative charged fraction depends on the positive charged fraction and vice versa. Equations (4.1) and (4.2) are simple to solve numerically for given values of the growth rate and the initial charged fractions, if the growth rate is assumed to be independent of the particle size.

Let us assume that we have measured or simulated data points of the charged fraction as a function of diameter. By iteratively changing the values of the growth rate and the initial charged fractions when solving Eqs. (4.1) and (4.2), we can search for the best

correspondence between the data points and the calculated values. As a result, estimates on the particle growth rate and the initial charged fractions are obtained. In this thesis, this method is denoted as the iteration method.

The iteration method in charge asymmetric framework was used to determine the growth rate from the charging states measured with Ion-DMPS instrument (Laakso et al., 2007a, and also Iida et al., 2006) at Helsinki, Finland, between December 2008 and February 2010 (**Paper III**). The growth rates determined with the method were much more consistent, when the asymmetric framework was used instead of the symmetric one. However, the growth rates from the iteration method were systematically higher than corresponding growth rates obtained using methods based on the evolution of the particle number size distribution.

The iteration method was also tested on a set of simulations in order to test how well the method was able to determine the growth rate and initial charged fraction, which were known for the simulations (**Paper IV**). It was found, that even rather small asymmetry in the small ion concentrations should be taken into account when using the iteration method (**Papers III** and **IV**). Also, the iteration method was found to be able to provide trustworthy estimates of the growth rate and initial charged fraction only if the growth rate was at least ~3 nm h^{-1}, provided that the charged particles did not grow much more rapidly than the neutral ones (**Paper IV**). For growth rates smaller than this, the initial charged fraction cannot be determined because of the loss of information as explained earlier in this section. The determination of small growth rates using the iteration method is difficult because in those situations the charged fractions approach the equilibrium value rapidly and follow the equilibrium closely. The growth rate is essentially determined from the divergence between the charged fraction and the equilibrium charged fraction, but in the case of small growth rates, the divergence is often caused by processes not taken into account in the method, which causes misinterpretation of the growth rate. Furthermore, it was found that the particle concentrations can easily be so high in atmospheric conditions that the coagulation processes, especially intramodal recombination, need to be taken into account when applying the method.

4.2 Definition of the aerosol charging state and fitting method

The aerosol charging state, *S*, is defined as a ratio of the charged fraction to the equilibrium charged fraction (Kerminen et al., 2007)

$$S^{\pm}\left(d_{\mathrm{p}}\right)=\frac{f^{\pm}\left(d_{\mathrm{p}}\right)}{f_{\mathrm{eq}}^{\pm}\left(d_{\mathrm{p}}\right)}. \tag{4.3}$$

Now, a particle population is under- or overcharged, if the charging state is below or above unity, respectively. Similarly to the charged fraction discussed in Section 4.1, the charging state approaches unity and at some point the information of the initial charging state is lost (Figure 6). Also, the charged fraction crossing the equilibrium value is the same as charging state dropping below unity, which was first observed in measurements (Laakso et al., 2007a) and then explained via theoretical analysis (Kerminen et al., 2007). In **Paper II**, the same phenomenon was reproduced in an aerosol dynamics simulation.

In their analysis, Kerminen et al. (2007) derived an analytical function that describes the behaviour of charging state as a function of diameter by making several simplifying assumptions. In the charge symmetric framework, the charging state is given by

$$S(d_\mathrm{p}) = 1 - \frac{1}{Kd_\mathrm{p}} + \frac{(S_0 - 1)Kd_0 + 1}{Kd_\mathrm{p}} \exp\left(-K(d_\mathrm{p} - d_0)\right) \tag{4.4}$$

where

$$K = \frac{\alpha N_\mathrm{C}}{\mathrm{GR}}. \tag{4.5}$$

Here N_C, α and GR are the small ion concentration (assumed to be the same for negative and positive ions), the recombination coefficient and the growth rate, respectively. The growth rate is assumed to be independent of the size or charge of the particles, α is assumed to be constant and S_0 is the value of the charging state at the size d_0. Furthermore, the equilibrium charged fraction is assumed to be given by

$$f_\mathrm{eq}(d_\mathrm{p}) \approx \frac{\beta(d_\mathrm{p})}{\alpha + 2\beta(d_\mathrm{p})} \approx \frac{\beta(d_\mathrm{p})}{\alpha}. \tag{4.6}$$

In previous studies, the initial charging state, S_0, has been determined from the measured values of charging state by fitting Eq. (4.4) to the measured values of the charging state by using S_0 and K as the fitting parameters (Laakso et al., 2007a, b; Gagné et al., 2008, 2010). The initial charged fraction is then calculated according to Eq. (4.3) with the assumption that f_eq can be estimated according to Wiedensohler (1988). In this thesis, this procedure is denoted as the fitting method.

In the work of this thesis, the theoretical analysis by Kerminen et al. (2007) was revised without assuming that the negative and positive small ion concentrations as well as concentrations of negative and positive particles are the same (**Paper III**). In that case, the charging state as a function of diameter can be written as

$$S^{\pm}(d_{\mathrm{p}}) = 1 - \frac{1}{K^{\pm} d_{\mathrm{p}}} + \frac{(S_0^{\pm} - 1) K^{\pm} d_0 + 1}{K^{\pm} d_{\mathrm{p}}} \exp\left(-K^{\pm}(d_{\mathrm{p}} - d_0)\right) \tag{4.7}$$

where

$$K^{\pm} = \frac{\alpha N_{\mathrm{C}}^{\mp}}{\mathrm{GR}} \tag{4.8}$$

Here, it should be noted that the parameter $K^{\pm}$ depends on the concentration of oppositely-charged small ions. Also, the equilibrium charged fraction is now assumed to be given by

$$f_{\mathrm{eq}}^{\pm}(d_{\mathrm{p}}) \approx \frac{\beta^{\pm}(d_{\mathrm{p}}) \times N_{\mathrm{C}}^{\pm}}{\alpha^{\mp} \times N_{\mathrm{C}}^{\mp} + \beta^{\pm}(d_{\mathrm{p}}) \times N_{\mathrm{C}}^{\pm} + \frac{\alpha^{\mp}}{\alpha^{\pm}} \beta^{\mp}(d_{\mathrm{p}}) \frac{(N_{\mathrm{C}}^{\mp})^2}{N_{\mathrm{C}}^{\pm}}} \approx \frac{\beta^{\pm}(d_{\mathrm{p}}) \times N_{\mathrm{C}}^{\pm}}{\alpha \times N_{\mathrm{C}}^{\mp}}. \tag{4.9}$$

In **Paper III**, we analysed the initial charging states from measured data using the fitting method with both symmetric and asymmetric small ion concentrations. The obtained values of initial charging state were quite similar regardless of the symmetric or asymmetric framework, but the values of K from different polarities were much closer to each other, when the asymmetric values were used. According to Eq. (4.8), the value of K for different polarities should be different only because of the difference in negative and positive small ion concentrations, which is by far too small to explain the difference observed in the values of K obtained using the fitting method. As a consequence, the fitting method captured the dynamics of the measured conditions much better when the asymmetric small ion concentrations were used instead of the symmetric ones.

The fitting method was also tested on a set of simulations in order to test how well the method was able to determine the growth rate and initial charged fraction, which were known for the simulations (**Paper IV**). As with the iteration method discussed in Section 4.1, the growth rate of at least ~3 nm h^{-1} was needed for the fitting method to provide reasonable estimates on the initial charged fraction and growth rate. The reason for this was, again, the loss of information before the particles reached the diameter range from which the analysed data were taken. Oppositely to the iteration method, however, the fitting method took into account the processes dominating the changes in the charged fraction in vast majority of the simulations. This is because the iteration method only took into account the ion-aerosol attachment, while the fitting method took into account also the intramodal recombination. As a drawback though, various processes can easily be added to the iteration method, whereas the fitting

method is not that flexible. In the case of the iteration method, the addition of new processes can be achieved by adding new terms into Eqs. (4.1) and (4.2), which makes the solving of the differential equations more laborious, but not much more difficult. On the other hand, in the case of the fitting method, any additional terms due to added processes would probably make it impossible to obtain an analytical solution like the one given in Eq. (4.7).

4.3 Implications to analysis of measurement data

Ion-DMPS is an instrument that has been designed to measure the aerosol charging state (Laakso et al., 2007a and also Mäkelä et al., 2001; Iida et al., 2006). The principle idea of the Ion-DMPS is the following: First, an air sample goes through a neutraliser that can be set to either push the sample to the equilibrium charging state or to not affect it at all. Then, the particles carrying a charge are size-segregated according to their mobility after which the amount of particles in each size section is counted. Thus, the instrument has four modes of operation as it measures either negative or positive particles that are either at the charge equilibrium or at the ambient charged fraction. The charging state is then obtained as the ratio of the amount of ambient charged particles to the corresponding value at charge equilibrium.

The equilibrium charged fraction in a neutraliser depends on the mass and mobility of the ions in the neutraliser and thus the equilibrium charged fraction in the neutraliser may differ between different ambient conditions (Reischl et al., 1996). For the sake of simplicity, the equilibrium charged fraction is typically estimated using the experimental parameterization according to Wiedensohler (1988) which has been observed to correspond well with experimental data even in sizes down to a few nanometres (Reischl et al., 1996). However, the concentrations of negative and positive small ions are relatively close to each other in the neutralizer, which is typically not the case in the ambient air (Hirsikko et al., 2011). In other words, the charging state measured with the Ion-DMPS may not actually represent the ambient charging state. In the previous section it was shown that the equilibrium charged fraction depends on the small ion concentrations according to Eq. (4.9). Now, the asymmetry in the small ion concentrations can be taken into account by scaling the charging state measured with the Ion-DMPS, $S_{\text{Ion-DMPS}}^{\pm}$, using the small ion concentrations (**Paper III**):

$$S_{\text{ambient}}^{\pm} = S_{\text{Ion-DMPS}}^{\pm} \frac{N_{\text{C}}^{\mp}}{N_{\text{C}}^{\pm}}, \tag{4.10}$$

where $S_{\text{ambient}}^{\pm}$ is the charging state in the ambient air. The fitting method described in Section 4.2 should then be used on the values of $S_{\text{ambient}}^{\pm}$ in order to obtain $S_0^{\pm}$ and $K^{\pm}$ that represent the ambient conditions (**Paper III**).

The procedure above takes into account only the effect of asymmetric small ion concentrations on the equilibrium charged fraction. However, also the mobilities of small ions and coagulation processes affect the equilibrium charged fraction. In principle, $S_{\text{ambient}}^{\pm}$ is then given by

$$S_{\text{ambient}}^{\pm} = S_{\text{Ion-DMPS}}^{\pm} \frac{f_{\text{Ion-DMPS}}^{\pm}}{f_{\text{ambient}}^{\pm}}, \tag{4.11}$$

where $f_{\text{Ion-DMPS}}^{\pm}$ and $f_{\text{ambient}}^{\pm}$ are the equilibrium values of the charging state in the neutralizer of Ion-DMPS and in the ambient air, respectively. The value of $f_{\text{Ion-DMPS}}^{\pm}$ can be estimated according to Wiedensohler (1988) while the value of $f_{\text{ambient}}^{\pm}$ should be estimated according to the specific ambient conditions. To achieve the latter, we first estimate the change rate of the charged fraction according to various processes (**Paper IV**):

$$\frac{df^{\pm}}{dt} = \left(\frac{df^{\pm}}{dt}\right)_{\text{IA}} + \left(\frac{df^{\pm}}{dt}\right)_{\text{REC}} + \left(\frac{df^{\pm}}{dt}\right)_{\text{SC}} + \left(\frac{df^{\pm}}{dt}\right)_{\text{CS}} \tag{4.12}$$

where subscript IA, REC, SC and CS refer to ion-aerosol attachment, intramodal recombination, self-coagulation excluding the intramodal recombination and coagulation scavenging. By approximating the nucleation mode using a monodisperse distribution, the different terms in Eq. (4.12) can be written as (**Paper IV**):

$$\left(\frac{df^{\pm}}{dt}\right)_{\text{IA}} = \beta^{\pm} N_{\text{C}}^{\pm}\left(1 - f^{-} - f^{+}\right) - \alpha^{\mp} N_{\text{C}}^{\mp} f^{\pm} \tag{4.13}$$

$$\left(\frac{df^{\pm}}{dt}\right)_{\text{REC}} = -k_{-,+} f^{\pm} f^{\mp} N_{\text{tot}}\left(1 - f^{\pm}\right) \tag{4.14}$$

$$\left(\frac{df^{\pm}}{dt}\right)_{\text{SC}} = N_{\text{tot}} f^{\pm}\left(1 - f^{-} - f^{+}\right)\left(\frac{1}{2} k_{0,0}\left(1 - f^{-} - f^{+}\right) + k_{0,-} f^{-} + k_{0,+} f^{+}\right) \tag{4.15}$$

$$\left(\frac{df^{\pm}}{dt}\right)_{\text{CS}} = -\text{CoagS}_{\pm} f^{\pm}\left(1 - f^{\pm}\right) + \text{CoagS}_{\mp} f^{+} f^{-} + \text{CoagS}_{0} f^{\pm}\left(1 - f^{-} - f^{+}\right) \tag{4.16}$$

where N_{tot} is the total concentration of nucleation mode particles. Now, we could combine Eqs. (4.12)–(4.16) and set $df^{\pm}/dt = 0$, since the total change rate is zero in the charge equilibrium. By doing this, we would obtained two equations, one for each

polarity, that would depend only on the negative and positive equilibrium charged fractions, total concentration of nucleation mode particles and the values of coagulation sink for negative, positive and neutral particles. The values of $f_{\text{ambient}}^{\pm}$ would then be obtained by solving those equations, provided that N_{tot}, CoagS_-, CoagS_+ and CoagS_0 could be obtained from the measurements.

The value of the charged fraction in the ambient charge equilibrium depends on the particle diameter due to numerous reasons. In the simplest approximation, given in Eq. (4.6), the diameter dependence of the equilibrium charged fraction comes only from the diameter dependence of the attachment coefficient, since the recombination coefficient was assumed to be constant. However, the recombination coefficient is not constant (Figure 2) and a more detailed consideration of the recombination coefficient could affect the equilibrium charged fraction significantly, even when processes other than ion-aerosol attachment are neglected. The more detailed approximation, given in Eqs. (4.12)–(4.16), indicates that the coagulation processes, which occur on a diameter dependent rate, could also affect the equilibrium charged fraction. In the sizes close to the particle formation, $d_{\text{p}} \leq 2$ nm, the exact values of these coefficients become very difficult to determine and measurements verifying these values are limited. Furthermore, in the analysis discussed above, it has been assumed that the small ions and particles are two separate groups and that the recombination products are stable. However, in sizes below 2 nm, either or both of these two assumptions may not hold.

In the work of this thesis, the iteration method took into account only the changes in the charged fraction by ion-aerosol attachment, while the fitting method took into account also the intramodal recombination. By using Eqs. (4.13)–(4.16), it can be estimated whether these are the dominating processes or not. The fraction of the total change rate of the charged fraction taken into account in the iteration and the fitting methods, $F_{\text{iter}}^{\pm}$ and $F_{\text{fit}}^{\pm}$, respectively, are given by (**Paper IV**):

$$F_{\text{iter}}^{\pm}\left(d_{\text{p}}\right) = \frac{\left|\left(\frac{df^{\pm}}{dt}\right)_{\text{IA}}\left(d_{\text{p}}\right)\right|}{\left|\left(\frac{df^{\pm}}{dt}\right)_{\text{IA}}\left(d_{\text{p}}\right)\right| + \left|\left(\frac{df^{\pm}}{dt}\right)_{\text{REC}}\left(d_{\text{p}}\right)\right| + \left|\left(\frac{df^{\pm}}{dt}\right)_{\text{CS}}\left(d_{\text{p}}\right)\right| + \left|\left(\frac{df^{\pm}}{dt}\right)_{\text{SC}}\left(d_{\text{p}}\right)\right|} \tag{4.17}$$

and

$$F_{\mathrm{fit}}^{\pm}\left(d_{\mathrm{p}}\right)=\frac{\left|\left(\frac{df^{\pm}}{dt}\right)_{\mathrm{IA}}\left(d_{\mathrm{p}}\right)\right|+\left|\left(\frac{df^{\pm}}{dt}\right)_{\mathrm{REC}}\left(d_{\mathrm{p}}\right)\right|}{\left|\left(\frac{df^{\pm}}{dt}\right)_{\mathrm{IA}}\left(d_{\mathrm{p}}\right)\right|+\left|\left(\frac{df^{\pm}}{dt}\right)_{\mathrm{REC}}\left(d_{\mathrm{p}}\right)\right|+\left|\left(\frac{df^{\pm}}{dt}\right)_{\mathrm{CS}}\left(d_{\mathrm{p}}\right)\right|+\left|\left(\frac{df^{\pm}}{dt}\right)_{\mathrm{SC}}\left(d_{\mathrm{p}}\right)\right|}. \quad (4.18)$$

Here the absolute values are used to limit the value of $F^{\pm}$ from zero to unity with a value close to unity meaning that the method takes into account the dominating processes. It is recommended to check the values of $F^{\pm}$ for the specific conditions before applying the iteration and/or the fitting method to measured data.

Now, the value of $F^{\pm}$ depends on the particle diameter. While it could be worthwhile to check the value of $F^{\pm}$ as a function of diameter separately for each case, it can be laborious when a large data set needs to be analysed. The procedure can be automated by checking that a representative value of $F^{\pm}$ for each case is below a predefined threshold value, 0.8 for example. One way of obtaining the representative value is to calculate the weighted average value of $F^{\pm}$ over a predefined diameter range using the total change rate of charged fraction as the weighting factor. In this case, the representative values, $F_{\mathrm{iter}}^{\pm}$ and $F_{\mathrm{fit}}^{\pm}$, can be written as (**Paper IV**)

$$F_{\mathrm{iter}}^{\pm}=\frac{\sum_{i=n}^{m}\left|\left(\frac{df^{\pm}}{dt}\right)_{\mathrm{IA}}\left(d_{\mathrm{p}}^{i}\right)\right|\times\left(\frac{df^{\pm}}{dt}\right)_{\mathrm{TOT}}\left(d_{\mathrm{p}}^{i}\right)}{\sum_{i=n}^{m}\left(\frac{df^{\pm}}{dt}\right)_{\mathrm{TOT}}\left(d_{\mathrm{p}}^{i}\right)} \quad (4.19)$$

and

$$F_{\mathrm{fit}}^{\pm}=\frac{\sum_{i=n}^{m}\left(\left|\left(\frac{df^{\pm}}{dt}\right)_{\mathrm{IA}}\left(d_{\mathrm{p}}^{i}\right)\right|+\left|\left(\frac{df^{\pm}}{dt}\right)_{\mathrm{REC}}\left(d_{\mathrm{p}}^{i}\right)\right|\right)\times\left(\frac{df^{\pm}}{dt}\right)_{\mathrm{TOT}}\left(d_{\mathrm{p}}^{i}\right)}{\sum_{i=n}^{m}\left(\frac{df^{\pm}}{dt}\right)_{\mathrm{TOT}}\left(d_{\mathrm{p}}^{i}\right)} \quad (4.20)$$

where the chosen diameter range is covered by the diameters from d_{p}^{n} to d_{p}^{m} in the diameter grid of the measurements. Using unweighted average of $F^{\pm}(d_{\mathrm{p}})$ is not recommended, since that value could be biased by the values of $F^{\pm}(d_{\mathrm{p}})$ observed at the diameters in which the total change rate is very small.

4.4 Ion-induced nucleation, initial charged fraction and apparent formation rates of neutral and charged particles

In the beginning of Section 4, it was stated that the initial fraction of charged particles depends on the fraction of particles formed carrying a charge, i.e. via ion-induced nucleation, IIN. However, the initial charged fraction is based on the concentrations of the neutral and charged particles over a diameter range that includes the size at which the particle formation is assumed to occur. The concentrations depend on sources of the particles into that diameter range and on the removal of particles out of that range. The sources into the diameter range are the particle formation and coagulation during which the diameter of the resulting particle is within this diameter range. The removal of particles out of the diameter range constitutes of the coagulation sink (both intramodal and scavenging by larger particles) and the growth of particles to sizes larger than the upper boundary of the diameter range.

The coagulation coefficient between two particles depends on the charges of those particles with the following order from smallest to highest: two similarly-charged particles, two neutral particles, a neutral and a charged particle and two oppositely-charged particles (Figure 2). In **Paper IV**, it was shown that the higher removal rate of charged vis-à-vis neutral particles by coagulation processes could lead to an underestimation of up to a factor of 2, when the fraction of IIN is estimated directly from the initial charged fraction. Furthermore, when the charged particles grow more rapidly than the neutral ones, the removal of charged particles due to growth over the upper boundary of the diameter range is higher than that of the neutral ones. In that case, the fraction of IIN is further underestimated. The magnitude of underestimation depends on the value of the enhancement factor, ξ, which in turn depends on the particle size (Nadykto and Yu, 2003; Lushnikov and Kulmala, 2004) as shown in Figure 4. In the conditions in which the coagulation processes are negligible, the relation between the fraction of IIN and the initial charged fraction can be written as (**Paper IV**):

$$\mathrm{IIN}^{\pm} = \frac{J_d^{\pm}}{J_d^{\mathrm{tot}}} = \frac{\mathrm{GR}_d^{\pm} n_d^{\pm}}{\mathrm{GR}_d^{0} n_d^{0} + \mathrm{GR}_d^{\pm} n_d^{-} + \mathrm{GR}_d^{\pm} n_d^{+}} = \frac{\xi n_d^{\pm}}{n_d^{0} + \xi\left(n_d^{-} + n_d^{+}\right)}, \tag{4.21}$$

where J_d^{tot}, $J_d^{\pm}$, GR_d^q and n_d^q are the apparent total formation rate of particles, apparent formation rate of charged particles, particle diameter growth rate and particle number size distribution, $n = dN/dd_{\mathrm{p}}$. Here d denotes the diameter in which the particle formation is assumed to occur and q denotes the charge of the particle.

An alternative way of estimating the proportion of IIN is to estimate the apparent formation rates of total and charged particles in the size in which the particles are

assumed to be formed (Kulmala et al., 2007). The apparent formation rate of particles at 1.8 nm size, $J_{1.8}^{\mathrm{tot}}$, can be written for total (neutral plus charged) particles as (Kulmala et al., 2007)

$$J_{1.8}^{\mathrm{tot}} = \frac{dN_{\mathrm{tot}}^{1.8-3}}{dt} + \mathrm{CoagS}^{1.8-3} \times N_{\mathrm{tot}}^{1.8-3} + \frac{p}{1.2\ \mathrm{nm}} \mathrm{GR}_3 N_{\mathrm{tot}}^{1.8-3} \tag{4.22}$$

and for charged particles as

$$\begin{aligned} J_{1.8}^{\pm} = {} & \frac{dN_{\pm}^{1.8-3}}{dt} + \mathrm{CoagS}^{1.8-3} \times N_{\pm}^{1.8-3} + \frac{p}{1.2\ \mathrm{nm}} \mathrm{GR}_3 N_{\pm}^{1.8-3} \\ & + \alpha^{\mp} N_{\pm}^{1.8-3} N_{\mp}^{<3} - \beta^{\pm} N_0^{1.8-3} N_{\pm}^{<1.8} \end{aligned} . \tag{4.23}$$

Here $N_{\mathrm{tot}}^{1.8-3}$, $N_q^{1.8-3}$ and $N_{\pm}^{<d}$ are the total concentration of 1.8–3 nm particles, concentrations of 1.8–3 nm particles with q charges and concentrations of charged particles with diameter smaller than d given in nm, respectively, and $\mathrm{CoagS}^{1.8-3}$ is the average coagulation sink of 1.8–3 nm particles. The factor p represents the proportion of the 1.8–3 nm particles that are activated for growth and the value of p is typically assumed to be unity (Kulmala et al., 2007). Assuming that the particles are formed with diameter of 1.8 nm, the proportion of IIN can be estimated as $(J_{1.8}^{-} + J_{1.8}^{+})/J_{1.8}^{\mathrm{tot}}$. The advantage of this method over estimating the proportion of IIN from the initial charged fractions is that this method takes into account the difference in the coagulation losses of neutral and charged particles. Nevertheless, it does not take into account the difference in the growth rates of neutral and charged particles and, furthermore, the growth rate is assumed to be constant over the diameter range from 1.8 to 3 nm. Also, the particle growth rate has to be determined with a separate method, which introduces yet another source of uncertainty.

5 Review of the papers and author's contribution

I am solely responsible for writing the introductory part of this thesis.

Paper I investigates the role of particle charges in the growth of freshly-formed particle population. Simple analytical formulae for estimating the growth rate due to self-coagulation and the apparent growth due to scavenging by larger pre-existing particles are provided. The growth rates due to different processes are analyzed from simulations conducted using the Ion-UHMA model. A few numerical issues related to simulating the condensational growth using a sectional model are examined. Charged particles are found to increase the growth rate due to both self-coagulation and coagulation scavenging by a factor of 1.5 to 2. It is shown that the higher condensational growth rate of charged particles compared to that of the neutral ones could considerably increase the growth rate of the particle population in sizes < ~5 nm. I am responsible for conducting the simulations, developing the new data-analysis methods, analyzing the simulated data and writing most of the paper.

Paper II introduces the new aerosol dynamics model, Ion-UHMA, which simulates the dynamics of both the neutral and charged particles. The model is shown to be capable of reproducing the measured time evolution of a particle number size distribution during a new particle formation event. Several possible future applications of the Ion-UHMA are presented. I am responsible for developing parts of the model, testing the model, conducting the simulations, analysing the simulated data and writing most of the paper.

Paper III investigates the proportion of IIN in urban conditions at Helsinki, Finland. The concentrations of negative and positive small ions are found to be different leading to introduction of a charge asymmetric framework. The data-analysis methods used to determine the growth rate and proportion of IIN from aerosol charging state are adapted to the charge asymmetric framework. The fraction of IIN, in the measured conditions, is found to be small (< 2 %). I am responsible for deriving the equations describing the behaviour of aerosol charging state in the charge asymmetric framework, analysing the particle growth rates from the measured charged fractions and writing parts of the paper.

Paper IV studies the situations in which the growth rate and proportion of IIN can be determined from the aerosol charging state using the data-analysis methods applied in **Paper III**. A set of simulations covering a wide range of atmospheric conditions is conducted using Ion-UHMA model. The methods are used on the simulated data and the results are compared to the values obtained directly from the model. The methods are found to be able to provide reasonable estimates when the particle growth rate is

above ~3 nm h^{-1} and, if the condensational growth rate of charged particles is of the same order of magnitude as that of the neutral ones. It is shown that the measurements close to the formation size of the particles are important when determining the proportion of IIN. A simple procedure for assessing the suitability of the data-analysis methods for particular measurement conditions is also provided. I am responsible for conducting the simulations, analysing the simulated data, deriving the assessment procedure and writing the paper.

6 Conclusions

The main focus of this thesis has been on getting better understanding on and new scientific insight into the dynamics of neutral and, especially, charged nucleation mode particles. A new model, Ion-UHMA, which simulates the dynamics of neutral and charged aerosol particles, has been developed for this purpose (**Paper II**). The model has been shown to be capable of reproducing the time evolution of the neutral and charged particle number size distributions during a new particle formation event as observed in the field measurements (**Paper II**). The Ion-UHMA has been used to provide data for testing previously used and newly developed data-analysis methods (**Paper I** and **IV**).

The charges of the aerosol particles were found to affect the growth rate of a nucleation mode in various ways. The average growth rate of the freshly formed particles could be significantly increased due to enhanced condensation onto charged particles (**Paper I**). The magnitude of this effect, however, is very dependent on the proportion of particles formed via IIN and on the concentration of small ions. Nevertheless, the increase in average growth rate could also have a significant effect on the concentration of particles reaching larger sizes, as the smallest particles are most vulnerable to removal due to coagulation scavenging.

The charged particles were found to increase the growth rate of the nucleation mode due to self-coagulation by up to a factor of 2 (**Paper I**). However, under most atmospheric conditions, the growth due to self-coagulation is so small compared to the growth due to condensation that neglecting the effect of charged particles on self-coagulation makes little difference on the total growth rate. The apparent growth due to coagulation scavenging was also found to increase when charged particles are taken into account (**Paper I**). The magnitude of the growth due to coagulation scavenging is very case dependent, but could be significant in sizes below ~10 nm in diameter. In the case of growth due to coagulation scavenging being significant, also the effect of charged particles, a factor of ~1.7 on average, is considerable.

The negative and positive small ion concentrations were observed to be different in the measurements conducted at Helsinki, Finland (**Paper III**). It was found out that even a rather small asymmetry in the small ion concentrations has a significant effect on the behaviour of aerosol charging state and fraction of charged particles as a function of diameter. This effect is most pronounced in the case of the charging state, which does not approach unity, if the asymmetry exists but is not taken into account (**Paper III**). In the work of this thesis, previous methods that have been used to analyse measured charging states and charged fractions were adapted to take into account the asymmetry in small ion concentrations (**Paper III**).

When testing the aforementioned methods on simulated data, it was found that the methods were able to give much more reliable estimates on the particle growth rate and proportion of IIN, if the asymmetry in small ion concentrations was taken into account (**Paper IV**). However, there are two issues limiting the applicability of these methods:

1) The particle growth rate has to be sufficiently high. When the growth rate is small, the information of the initial charged fraction may be lost before the particles reach measurable sizes. The value of the growth rate that is needed for the methods to give reliable estimates of IIN is ambiguous, as it depends on the concentrations of small ions and the size range of the measurements. Under the conditions used in the simulations in **Paper IV**, the methods were found to give unreliable estimates when the growth rate was smaller than ~3 nm h^{-1}.

2) The methods should take into account the processes that cause the changes in the charged fraction. In the work of this thesis, the fitting method took into account the ion-aerosol attachment and intramodal recombination, whereas the iteration method only took into account the ion-aerosol attachment. In atmospheric conditions, the ion-aerosol attachment is typically the dominating process, while the effect of coagulation processes increase with increasing particle number concentration. The nucleation mode concentrations can easily be high enough for the intramodal recombination to have a significant effect on the charged fraction.

Both of these issues should be considered separately for each case before applying the methods on measured data.

This thesis describes the dynamics of neutral and charged particles with a main focus on analysing new particle formation events. Two major questions yet unanswered in this regard are the proportion of particles formed via IIN and to what extent does the particle diameter growth rate depend on the size and charge of the particle. However, recent developments in measurement instrumentation and theoretical approaches suggest that these questions could be answered in the near future.

As a direct continuation of the work of this thesis, many currently used data-analysis methods could be tested on the simulated data using a similar approach to the one used in **Paper IV**. Methods suitable for this kind of study are, for example, the method used to determine the proportion of IIN from the apparent formation rates of neutral and charged particles and the methods used to determine the diameter growth rate from the evolution of particle number size distribution. The study on the methods used to determine the growth rate would also provide information on how well the growth rate determined from the population of charged particles describes the growth rate of the total particle population.

Nomenclature

Of attachment and recombination

The definitions related to the attachment and recombination processes that are used in this thesis are the following. Ion-aerosol attachment refers to the attachment of small ions to neutral or oppositely-charged particles with the attachment to similarly-charged particles omitted. Ion-ion recombination refers to recombination of oppositely-charged small ions. Intramodal recombination refers to coagulation between oppositely-charged nucleation mode particles. Attachment coefficient refers to collision efficiency in the attachment of small ions to neutral particles and recombination coefficient refers to collision efficiency in the attachment of small ions to oppositely-charged particle, whereas ion-ion recombination coefficient refers to collision efficiency in recombination between two oppositely-charged small ions.

Terminology

Asymmetric small ion concentrations: concentrations of negative and positive small ions may have different values

Charge asymmetric framework: Concentrations of negative and positive small ions, as well as concentrations of negative and positive particles, are allowed have different values. Also, the attachment and recombination coefficients of negative and positive small ions are allowed to have different values.

Charge equilibrium: a state in which the neutralization of charged particles and charging of neutral particles are at balance in a given particle size

Charge symmetric framework: Concentrations of negative and positive small ions, as well as concentrations of negative and positive particles, are assumed to be the same. Also, the attachment and recombination coefficients of negative and positive small ions are assumed to be the same.

Charged fraction: the ratio of the concentration of charged particles to total particle concentration at a given particle size

Charging state: the ratio of the charged fraction to the charged fraction in charge equilibrium at a given particle size

Equilibrium charged fraction: the fraction of charged to total particles in the charge equilibrium at a given particle size

Initial charged fraction: the value of charged fraction at the size where the particle formation occurs

Initial charging state: the value of charging state at the size where the particle formation occurs

Small ion: a large molecule or a molecular cluster carrying a positive or a negative electric charge and with a diameter smaller than that of the freshly-formed particles

Symmetric small ion concentrations: concentrations of negative and positive small ions are assumed to be the same

Symbols

The symbols used in the introductory part of this thesis are listed here. Some of the notations are slightly different in the research articles of this thesis and may also vary between different articles. The summation indices are not included in the list, but they are explicitly written in the corresponding equations. The symbols used only in the legends of the figures are not listed here. Using a single symbol for multiple purposes has been avoided, except in the following two cases: (1) J denotes molar flux onto particle surface in condensation and apparent formation rate of particles when discussing the proportion of ion-induced nucleation and (2) k without indices denotes Boltzmann constant while k with indices denotes coagulation coefficient.

a_{SA}	polarizability of sulphuric acid
c_{s}	saturation concentration of the condensing vapour at the particle surface
$c_{\mathrm{s}}^{\,0}$	saturation concentration of the condensing vapour over a flat surface
c_{∞}	concentration of the condensing vapour far away from the particle
CoagS^{i}	coagulation sink of particles in size section i
CoagS_{q}	coagulation sink of particles with charge q
$\mathrm{CoagS}_{q}^{\,i}$	coagulation sink of particles with charge q in size section i
$\mathrm{CoagS}^{1.8-3}$	coagulation sink of particles in the diameter range of 1.8–3 nm
$\mathrm{CoagS}^{\dagger}$	count mean value of the coagulation sink

$\mathrm{CoagS}^{\ddagger}$	count mean value of the coagulation sink averaged over three charge classes
d_p	particle diameter
$d_\mathrm{p}^{\,i}$	diameter of particles in size section i
$d_\mathrm{p}^{\,\dagger}$	count mean diameter
$d_\mathrm{p}^{\,\ddagger}$	count mean diameter averaged over three charge classes
d_SA	diameter of a sulphuric acid molecule
d_v	diameter of a vapour molecule
d_0	diameter in which the particles are assumed to be formed
D_p	diffusivity of a particle in the air
D_v	diffusivity of a vapour molecule in the air
e	elementary charge
E	auxiliary variable defined in Eq. (2.17)
$f_\mathrm{ambient}^{\pm}$	equilibrium charged fraction in the ambient conditions
f_eq	charged fraction in the charge equilibrium when the charged fractions of negative and positive particles are assumed to be the same
$f_\mathrm{eq}^{\pm}$	charged fraction in the charge equilibrium
$f_\mathrm{Ion\text{-}DMPS}^{\pm}$	equilibrium charged fraction in the neutralizer
$f^{\pm}$	charged fraction
$F_\mathrm{fit}^{\pm}$	fraction of the change rate of the charged fraction that is taken into account in the fitting method
$F_\mathrm{iter}^{\pm}$	fraction of the change rate of the charged fraction that is taken into account in the iteration method
$F^{\pm}$	fraction of the change rate of the charged fraction that is taken into account in a data-analysis method
GR	particle diameter growth rate
$\mathrm{GR}_\mathrm{cond}$	particle diameter growth rate due to condensation
$\mathrm{GR}_\mathrm{cond,c}$	growth rate due to condensation in the continuum regime

$GR_{cond,k1}$ growth rate due to condensation when assuming that the size of the molecule is negligible compared to that of the particle and that the thermal speed of the particle is negligible compared to that of the molecule

$GR_{cond,k2}$ growth rate due to condensation when the size of the molecule and the thermal speed of the particle are taken into account

GR_d growth rate of particles with diameter d given in nm

GR_d^q growth rate of particles with diameter d given in nm and charge q

GR_{eff} effective growth rate due to condensation when numerical errors have been taken into account

GR_{scav} growth rate of the count mean diameter of a particle population due to coagulation scavenging

GR_{scoag} growth rate of the diameter that represents a particle population due to self-coagulation

$IIN^{\pm}$ proportion of ion-induced nucleation

J_c molar flux onto a particle surface in the continuum regime

J_d^q apparent formation rate of particles with charge q and diameter d (in nm)

J_d^{tot} apparent total formation rate of particles with diameter d given in nm

J_{k1} molar flux onto a particle surface in the kinetic regime when assuming that the size of the molecule is negligible compared to that of the particle and that the thermal speed of the particle is negligible compared to that of the molecule

J_{k2} molar flux onto a particle surface in the kinetic regime when the size of the molecule and the thermal speed of the particle are taken into account

J_t molar flux onto a particle surface in the transition regime

k Boltzmann constant

$k_{q1,q2}$ coagulation coefficient between particles with charges q1 and q2

K parameter related to the behaviour of the charging state when the concentrations of negative and positive small ions and the concentrations of negative and positive particles are assumed to be the same

$K^{\pm}$ parameter related to the behaviour of the charging state when the concentrations of negative and positive small ions and the concentrations of negative and positive particles are not assumed to be the same

Kn	Knudsen number
l_{SA}	dipole moment of sulphuric acid
n_d^q	number size distribution of particles with diameter d (in nm) and charge q
N_C	concentration of small ions when the concentrations of negative and positive small ions are assumed to be the same
$N_C^{\pm}$	concentration of negative or positive small ions
N_q	concentration of particles with charge q
N_q^i	concentration of particles with charge q in size section i
$N_q^{1.8–3}$	concentration of 1.8–3 nm particles with charge q
N_{tot}	total particle concentration
N_{tot}^i	total particle concentration in size section i
$N_{tot}^{1.8–3}$	total concentration of 1.8–3 nm particles
$N_{\pm}^{<d}$	concentration of charged particles with diameter smaller than d given in nm
p	proportion of 1.8–3 nm particles that are activated for growth
q	number of charges in a particle (values "–" and "+" refer to a single negative and to a single positive charge, respectively)
Q	ion-pair production rate
r	distance of the charges when describing a polar molecule as a constituent with opposite charges set apart by a fixed distance
r_{SA}	distance of the charges of a sulphuric acid molecule
$R^{\pm}$	net removal rate of small ions via processes other than ion-ion recombination
S	charging state when the concentrations of the negative and positive small ions are assumed to be the same
$S_{ambient}^{\pm}$	charging state in the ambient conditions
$S_{Ion\text{-}DMPS}^{\pm}$	charging state measured with Ion-DMPS
S_0	charging state in the size where the particles are assumed to be formed when the concentrations of negative and positive small ions are assumed to be the same

$S_0^{\pm}$	charging state in the size where the particles are assumed to be formed
$S^{\pm}$	charging state
t	time
T	temperature
V_m	volume of a condensing molecule
$V_{m,l}$	volume of a condensing molecule in liquid phase
V_p	volume of a particle
z	auxiliary variable defined in Eq. (2.16)
$Z^{\pm}$	mobility of a small ion
α	ion-ion recombination coefficient
$\alpha^{\pm}$	recombination coefficient of a small ion to an oppositely-charged particle
β	attachment coefficient of a small ion to a neutral particle when the coefficient is assumed to be the same for negative and positive small ions
$\beta_{eff}^{\pm}$	effective ion-aerosol attachment coefficient of a small ion for polydisperse particle population
$\beta^{\pm}$	attachment coefficient of a small ion to a neutral particle
γ	molecular accommodation coefficient
γ_m	mass accommodation coefficient
ε_g	relative permittivity of vapour
ε_p	relative permittivity of a particle
ε_0	vacuum permittivity
η	correction factor that takes into account the continuum effects in the transition regime
λ	ratio between the diameters corresponding to consecutive size sections
v_p	mean thermal speed of a particle
v_v	mean thermal speed of a vapour molecule
ξ	growth enhancement factor of the charged particles
ξ_{LK}	growth enhancement factor according to Lushnikov and Kulmala (2004)

ξ_{NY} growth enhancement factor according to Nadykto and Yu (2003)

σ surface tension of the condensing compound

χ Fuchs-Sutugin transition regime correction factor

$(df^{\pm}/dt)_{CS}$ change rate of the charged fraction due to coagulation scavenging

$(df^{\pm}/dt)_{IA}$ change rate of the charged fraction due to ion-aerosol attachment

$(df^{\pm}/dt)_{REC}$ change rate of the charged fraction due to recombination of oppositely-charged nucleation mode particles

$(df^{\pm}/dt)_{SC}$ change rate of the charged fraction due to self-coagulation within the nucleation mode excluding intramodal recombination

$(df^{\pm}/dt)_{TOT}$ total change rate of the charged fraction

$(d_p \times \mathrm{CoagS})^{\dagger}$ count mean value of the diameter multiplied by the coagulation sink

$(d_p \times \mathrm{CoagS})^{\ddagger}$ count mean value of the diameter multiplied by the coagulation sink averaged over three charge classes

Acronyms

AEROION a previous model that simulates dynamics of neutral and charged particles (Laakso et al., 2002)

CCN cloud condensation nuclei

GCR galactic cosmic rays

IIN ion-induced nucleation

Ion-DMPS an instrument based on a Differential Mobility Particle Sizer, but modified to measure the concentrations of charged particles in ambient conditions and after a neutralizer; the instrument used in this thesis

Ion-UHMA University of Helsinki Multicomponent Aerosol model for neutral and charged particles; the model used in this thesis

UHMA University of Helsinki Multicomponent Aerosol model (Korhonen et al., 2004)

SMEAR II Station for Measuring Forest Ecosystem–Atmosphere Relations; located at the Hyytiälä Forestry Field Station of the University of Helsinki (61°51′ N, 24°17′ E, 181 m above sea level)

References

Aalto, P., Hämeri, K., Becker, E., Weber, R., Salm, J., Mäkelä, J. M., Hoell, C., O'dowd, C. D., Hansson, H.-C., Väkevä, M., Koponen, I. K., Buzorius, G., and Kulmala, M.: Physical characterization of aerosol particles during nucleation events, Tellus, 53B, 344–358, 2001.

Agee, E. M., Kiefer, K., and Cornett, E.: Relationship of lower troposphere cloud cover and cosmic rays: An updated perspective, J. Climate, 25, 1057–1060, 2012.

Albrecht, B. A.: Aerosols, cloud microphysics, and fractional cloudiness, Science, 245, 1227–1230, 1989.

Anderson, H. R.: Air pollution and mortality: A history, Atmos. Environ., 43, 142–152, 2009.

Anttila, T., Kerminen, V.-M., Kulmala, M., Laaksonen, A., and O'Dowd, C. D.: Modelling the formation of organic particles in the atmosphere, Atmos. Chem. Phys., 4, 1071–1083, 2004.

Arnold., F.: Multi-ion complexes in the stratosphere—implications for trace gases and aerosols, Nature, 284, 610–611, 1980.

Asmi, A., Wiedensohler, A., Laj, P., Fjaeraa, A.-M., Sellegri, K., Birmili, W., Weingartner, E., Baltensperger, U., Zdimal, V., Zikova, N., Putaud, J.-P., Marinoni, A., Tunved, P., Hansson, H.-C., Fiebig, M., Kivekäs, N., Lihavainen, H., Asmi, E., Ulevicius, V., Aalto, P. P., Swietlicki, E., Kristensson, A., Mihalopoulos, N., Kalivitis, N., Kalapov, I., Kiss, G., de Leeuw, G., Henzing, B., Harrison, R. M., Beddows, D., O'Dowd, C., Jennings, S. G., Flentje, H., Weinhold, K., Meinhardt, F., Ries, L., and Kulmala, M.: Number size distributions and seasonality of submicron particles in Europe 2008–2009, Atmos. Chem. Phys., 11, 5505–5538, 2011.

Carslaw, K. S., Harrison, R. G., and Kirkby, J.: Cosmic Rays, Clouds, and Climate, Science, 298, 1732–1737, 2002.

Dal Maso, M., Kulmala, M., Riipinen, I., Wagner, R., Hussein, T., Aalto, P. P., and Lehtinen, K. E. J.: Formation and growth of fresh atmospheric aerosols: eight years of aerosol size distribution data from SMEAR II, Hyytiälä, Finland, Boreal Env. Res., 10, 323–336, 2005.

de la Mora, J. F., Thomson, B. A., and Gamero-Castaño, M.: Tandem Mobility Mass Spectrometry Study of Electrosprayed Tetraheptyl Ammonium Bromide Clusters, J. Am. Soc. Mass Spectr., 16, 717–732, 2005.

de Leeuw, G., Andreas, E. L., Anguelova, M. D., Fairall, C. W., Lewis, E. R., O'Dowd, C., Schulz, M., and Schwartz, S. E.: Production flux of sea spray aerosol, Rev. Geophys., 49, RG2001, doi:10.1029/2010RG000349, 2011.

Després, V. R., Huffman, J. A., Burrows, S. M., Hoose, C., Safatov, A. S., Buryak, G., Fröhlich-Nowoisky, J., Elbert, W., Andreae, M. O., Pöschl, U., and Jaenicke, R.: Primary biological aerosol particles in the atmosphere: a review, Tellus, 64B, 15598, doi:10.3402/tellusb.v64i0.15598, 2012.

Donahue, N. M., Trump, E. R., Pierce, J. R., and Riipinen, I.: Theoretical constraints on pure vapor-pressure driven condensation of organics to ultrafine particles, Geophys. Res. Lett., 38, L16801, doi:10.1029/2011GL048115, 2011.

Ehn, M., Junninen, H., Petäjä, T., Kurtén, T., Kerminen, V.-M., Schobesberger, S., Manninen, H. E., Ortega, I. K., Vehkamäki, H., Kulmala, M., and Worsnop, D. R.: Composition and temporal behavior of ambient ions in the boreal forest, Atmos. Chem. Phys., 10, 8513–8530, 2010a.

Ehn, M., Vuollekoski, H., Petäjä, T., Kerminen, V.-M., Vana, M., Aalto, P., de Leeuw, G., Ceburnis, D., Dupuy, R., O'Dowd, C. D., and Kulmala M.: Growth rates during coastal and marine new particle formation in Western Ireland, J. Geophys. Res., 115, D18218, doi:10.1029/2010JD014292, 2010b.

Ehn, M., Junninen, H., Schobesberger, S., Manninen, H. E., Franchin, A., Sipilä, M., Petäjä, T., Kerminen, V.-M., Tammet, H., Mirme, A., Mirme, S., Hõrrak, U., Kulmala, M., and Worsnop, D. R.: An Instrumental Comparison of Mobility and Mass Measurements of Atmospheric Small Ions, Aerosol Sci. Technol, 45, 522–532, 2011.

Eisele, F. L.: Natural and anthropogenic negative ions in the troposphere, J. Geophys. Res., 94, D2, doi:10.1029/JD094iD02p02183, 1989.

Forster, P., Ramaswamy, V., Artaxo, P., Berntsen, T., Betts, R., Fahey, D. W., Haywood, J., Lean, J., Lowe, D. C., Myhre, G., Nganga, J., Prinn, R., Raga, G., Schulz, M., and Van Dorland, R.: Changes in Atmospheric Constituents and in Radiative Forcing. In: Climate Change 2007: The Physical Science Basis. Contribution of Working Group I to the Fourth Assessment Report of the Intergovernmental Panel on Climate Change [Solomon, S., D. Qin, M. Manning, Z.

Chen, M. Marquis, K.B. Averyt, M.Tignor and H.L. Miller (eds.)]. Cambridge University Press, Cambridge, United Kingdom and New York, NY, USA, 2007.

Fuchs, N. A.: The Mechanics of Aerosols, Pergamon Press, Oxford, England, pp. 408, 1964.

Fuchs, N. A., and Sutugin, A. G.: Highly dispersed aerosols. In: Hidy, G. M., and Brock, J. R. (eds.), Topics in current aerosol research, Pergamon Press, New York, USA, 1–60, 1971.

Gaffney, J. S., and Marley, N. A.: The impacts of combustion emissions on air quality and climate – From coal to biofuels and beyond, Atmos. Environ., 43, 23–36, 2009.

Gagné, S., Laakso, L., Petäjä, T., Kerminen, V.-M., and Kulmala, M.: Analysis of one year of Ion-DMPS data from the SMEAR II station, Finland, Tellus, 60B, 318–329, 2008.

Gagné, S., Nieminen, T., Kurtén, T., Manninen, H. E., Petäjä, T., Laakso, L., Kerminen, V.-M., Boy, M., and Kulmala, M.: Factors influencing the contribution of ion-induced nucleation in a boreal forest, Finland, Atmos. Chem. Phys., 10, 3743–3757, 2010.

Goldstein, A. E., and Galbally, I. E.: Known and Unexplored Organic Constituents in the Earth's Atmosphere, Environ. Sci. Technol., 41, 1514–1521, 2007.

Goto, D., Nakajima, T., Takemura, T., and Sudo, K.: A study of uncertainties in the sulfate distribution and its radiative forcing associated with sulfur chemistry in a global aerosol model, Atmos. Chem. Phys., 11, 10889–10910, 2011.

Gurjar, B. R., Jain, A., Sharma, A., Agarwal, A., Gupta, P., Nagpure, A. S., and Lelieveld, J.: Human health risks in megacities due to air pollution, Atmos. Environ., 44, 4606–4613, 2010.

Hand, J. L., and W. C. Malm: Review of aerosol mass scattering efficiencies from ground-based measurements since 1990, J. Geophys. Res., 112, D16203, doi:10.1029/2007JD008484, 2007.

Hari, P. and Kulmala, M.: Station for Measuring Ecosystem-Atmosphere Relations (SMEAR II), Boreal Env. Res., 10, 315–322, 2005.

Harrison, R. G., and Carslaw, K. S.: Ion-aerosol-cloud processes in the lower atmosphere, Rev. Geophys., 41, 1012, doi:10.1029/2002RG000114, 2003.

Harrison, R. G., and Tammet, H.: Ions in Terrestrial Atmosphere and Other Solar System Atmospheres, Space Sci. Rev., 137, 107–118, 2008.

Heyder, J, Gebhart, J, Rudolf, G, Schiller, C, and Stahlhofen, W.: Deposition of particles in the human respiratory tract in the size range 0.005–15 μm, J. Aerosol Sci., 17, 811–825, 1986.

Hirsikko, A., Laakso, L., Hõrrak, U., Aalto, P. P., Kerminen, V.-M., and Kulmala, M.: Annual and size dependent variation of growth rates and ion concentrations in boreal forest, Boreal Env. Res., 10, 357–369, 2005.

Hirsikko, A., Nieminen, T., Gagné, S., Lehtipalo, K., Manninen, H. E., Ehn, M., Hõrrak, U., Kerminen, V.-M., Laakso, L., McMurry, P. H., Mirme, A., Mirme, S., Petäjä, T., Tammet, H., Vakkari, V., Vana, M., and Kulmala, M.: Atmospheric ions and nucleation: a review of observations, Atmos. Chem. Phys., 11, 767–798, 2011.

Hoppel, W. A., and Frick, G. M.: Ion-Aerosol Attachment Coefficients and the Steady-State Charge Distribution on Aerosols in a Bipolar Ion Environment, Aerosol Sci. Technol., 5, 1–21, 1986.

Hoppel, W. A., and Frick, G. M.: The Nonequilibrium Character of the Aerosol Charge Distribution Produced by Neutralizers, Aerosol Sci. Technol., 12, 471–496, 1990.

Hoppel, W. A., Frick, G. M., and Fitzgerald, J. W.: Marine boundary layer measurements of new particle formation and the effects nonprecipitating clouds have on aerosol size distribution, J. Geophys. Res., 99, 14443–14459, 1994.

Hõrrak, U., Mirme, A., Salm, J., Tamm, E., and Tammet, H.: Air ion measurements as a source of information about atmospheric aerosols, Atmos. Res., 46, 233–242, 1998.

Hõrrak, U., Aalto, P. P., Salm, J., Komsaare, K., Tammet, H., Mäkelä, J. M., Laakso, L., and Kulmala, M.: Variation and balance of positive air ion concentrations in a boreal forest, Atmos. Chem. Phys., 8, 655–675, 2008.

Howard, J., Wersborg, B., and Williams, G.: Coagulation of carbon particles in premixed flames, Faraday Symp. Chem. Soc., 7, 109–119, 1973.

Huneeus, N., Schulz, M., Balkanski, Y., Griesfeller, J., Prospero, J., Kinne, S., Bauer, S., Boucher, O., Chin, M., Dentener, F., Diehl, T., Easter, R., Fillmore, D., Ghan, S., Ginoux, P., Grini, A., Horowitz, L., Koch, D., Krol, M. C., Landing, W., Liu, X., Mahowald, N., Miller, R., Morcrette, J.-J., Myhre, G., Penner, J., Perlwitz, J., Stier, P., Takemura, T., and Zender, C. S.: Global dust model intercomparison in AeroCom phase I, Atmos. Chem. Phys., 11, 7781–7816, 2011.

Iida, K., Stolzenburg, M. R., McMurry, P. H., Dunn, M. J., Smith, J. N., Eisele, F., and Keady, P.: Contribution of ion-induced nucleation to new particle formation: Methodology and its application to atmospheric observations in Boulder, Colorado, J. Geophys. Res., 111, d23201, doi:10.1029/2006JD007167, 2006.

Iida, K., Stolzenburg, M. R., McMurry, P. H. and Smith, J. N.: Estimating nanoparticle growth rates from size-dependent charged fractions: Analysis of new particle formation events in Mexico City, J. Geophys. Res., 113, D05207, doi:10.1029/2007JD009260, 2008.

Israël, H.: Atmospheric electricity, Vol. I., Israel Program for Scientific Translations, Jerusalem, pp. 317, 1970.

Israël, H.: Atmospheric electricity, Vol. II., Israel Program for Scientific Translations, Jerusalem, pp. 318–796, 1973.

Jacobson, M. Z., and Turco, R. P.: Simulating condensational growth, evaporation, and coagulation of aerosols using a combined moving and stationary size grid, Aerosol Sci. Technol., 22, 73–92, 1995.

Jacobson, M. Z.: Fundamentals of Atmospheric Modeling, Cambridge University Press, New York, USA, pp. 813, 2005.

Jaeglé, L., Quinn, P. K., Bates, T. S., Alexander, B., and Lin, J.-T.: Global distribution of sea salt aerosols: new constraints from in situ and remote sensing observations, Atmos. Chem. Phys., 11, 3137–3157, 2011.

Jimenez, J. L., Canagaratna, M. R., Donahue, N. M., Prevot, A. S. H., Zhang, Q., Kroll, J. H., DeCarlo, P. F., Allan, J. D., Coe, H., Ng, N. L., Aiken, A. C., Docherty, K. S., Ulbrich, I. M., Grieshop, A. P., Robinson, A. L., Duplissy, J., Smith, J. D., Wilson, K. R., Lanz, V. A., Hueglin, C., Sun, Y. L., Tian, J., Laaksonen, A., Raatikainen, T., Rautiainen, J., Vaattovaara, Ehn, M., Kulmala, M., Tomlinson, J. M., Collins, D. R., Cubison, M. J., Dunlea, E. J., Huffman, J. A., Onasch, T. B., Alfarra, M. R., Williams, P. I., Bower, K., Kondo, Y., Schneider, J., Drewnick, F., Borrmann, S., Weimer, S., Demerjian, K., Salcedo, D., Cottrell, L., Griffin, R., Takami, A., Miyoshi, T., Hatakeyama, S., Shimono, A.,Sun, J. Y., Zhang, Y. M., Dzepina, K., Kimmel, J. R., Sueper, D., Jayne, J. T., Herndon, S. C., Trimborn, A. M., Williams, R., Wood, E. C., Middlebrook, A. M., Kolb, C. E., Baltensperger, U., and Worsnop, D. R.: Evolution of organic aerosols in the atmosphere, Science, 326, 1525–1529, 2009.

Kerminen, V.-M., and Wexler, A. S.: Growth laws for atmospheric aerosol particles: An examination of the bimodality of the accumulation mode, Atmos. Environ., 29, 3263–3275, 1995.

Kerminen, V.-M., Pirjola, L., and Kulmala, M.: How significantly does coagulational scavenging limit atmospheric particle production?, J. Geophys. Res., 106, D20, doi:10.1029/2001JD000322, 2001.

Kerminen, V.-M., and Kulmala, M.: Analytical formulae connecting the "real" and the "apparent" nucleation rate and the nuclei number concentration for atmospheric nucleation events, J. Aerosol Sci., 33, 609–622, 2002.

Kerminen, V.-M., Lehtinen, K. E. J., Anttila, T., and Kulmala, M.: Dynamics of atmospheric nucleation mode particles: a timescale analysis, Tellus, 56B, 135–146, 2004.

Kerminen, V.-M., Anttila, T., Petäjä, T., Laakso, L., Gagné, S., Lehtinen, K. E. J., and Kulmala, M.: Charging state of the atmospheric nucleation mode: Implications for separating neutral and ion-induced nucleation, J. Geophys. Res., 112, D21205, doi:10.1029/2007JD008649, 2007.

Kerminen, V.-M., Petäjä, T., Manninen, H. E., Paasonen, P., Nieminen, T., Sipilä, M., Junninen, H., Ehn, M., Gagné, S., Laakso, L., Riipinen, I., Vehkamäki, H., Kurten, T., Ortega, I. K., Dal Maso, M., Brus, D., Hyvärinen, A., Lihavainen, H., Leppä, J., Lehtinen, K. E. J., Mirme, A., Mirme, S., Hõrrak, U., Berndt, T., Stratmann, F., Birmili, W., Wiedensohler, A., Metzger, A., Dommen, J., Baltensperger, U., Kiendler-Scharr, A., Mentel, T. F., Wildt, J., Winkler, P. M., Wagner, P. E., Petzold, A., Minikin, A., Plass-Dülmer, C., Pöschl, U., Laaksonen, A., and Kulmala, M.: Atmospheric nucleation: highlights of the EUCAARI project and future directions, Atmos. Chem. Phys., 10, 10829–10848, 2010.

Kirkby, J.: Cosmic Rays and Climate, Surv. Geophys., 28, 333–375, 2007.

Korhonen, P., Kulmala, M., Laaksonen, A., Viisanen, Y., McGraw, R., and Seinfeld, J. H.: Ternary nucleation of H_2SO_4, NH_3, and H_2O in the atmosphere, J. Geophys. Res., 104, D21, doi:10.1029/1999JD900784, 1999.

Korhonen, H., Lehtinen, K. E. J., and Kulmala, M.: Multicomponent aerosol dynamics model UHMA: model development and validation, Atmos. Chem. Phys., 4, 757–771, 2004.

Kuang, C., McMurry, P. H., McCormick, A. V., and Eisele, F. L.: Dependence of nucleation rates on sulfuric acid vapor concentration in diverse atmospheric locations, J. Geophys. Res., 113, D10209, doi:10.1029/2007JD009253, 2008.

Kuang, C., Chen, M., Zhao, J., Smith, J., McMurry, P. H. and Wang, J.: Size and time-resolved growth rate measurements of 1 to 5 nm freshly formed atmospheric nuclei, Atmos. Chem. Phys., 12, 3573–3589, 2012.

Kulmala, M., Kerminen, V.-M., Anttila, T., Laaksonen, A., and O'Dowd, C. D.: Organic aerosol formation via sulphate cluster activation, J. Geophys. Res., 109, D04205, doi:10.1029/2003JD003961, 2004a.

Kulmala, M., Laakso, L., Lehtinen, K. E. J., Riipinen, I., Dal Maso, M., Anttila, T., Kerminen, V.-M., Hõrrak, U., Vana, M., and Tammet, H.: Initial steps of aerosol growth, Atmos. Chem. Phys., 4, 2553–2560, 2004b.

Kulmala, M., Lehtinen, K. E. J., and Laaksonen, A.: Cluster activation theory as an explanation of the linear dependence between formation rate of 3 nm particles and sulphuric acid concentration, Atmos. Chem. Phys., 6, 787–793, 2006.

Kulmala, M., Riipinen, I., Sipilä, M., Manninen, H. E., Petäjä, T., Junninen, H., Dal Maso, M., Mordas, G., Mirme, A., Vana, M., Hirsikko, A., Laakso, L., Harrison, R. M., Hanson, I., Leung, C., Lehtinen, K. E. J., and Kerminen, V.-M.: Towards direct measurements of atmospheric nucleation, Science, 318, 89–92, 2007.

Kulmala, M., and Kerminen, V.-M.: On the formation and growth of atmospheric nanoparticles, Atmos. Res., 90, 132–150, 2008.

Kulmala, M., Asmi, A., Lappalainen, H. K., Baltensperger, U., Brenguier, J.-L., Facchini, M. C., Hansson, H.-C., Hov, Ø., O'Dowd, C. D., Pöschl, U., Wiedensohler, A., Boers, R., Boucher, O., de Leeuw, G., Denier van der Gon, H. A. C., Feichter, J., Krejci, R., Laj, P., Lihavainen, H., Lohmann, U., McFiggans, G., Mentel, T., Pilinis, C., Riipinen, I., Schulz, M., Stohl, A., Swietlicki, E., Vignati, E., Alves, C., Amann, M., Ammann, M., Arabas, S., Artaxo, P., Baars, H., Beddows, D. C. S., Bergström, R., Beukes, J. P., Bilde, M., Burkhart, J. F., Canonaco, F., Clegg, S. L., Coe, H., Crumeyrolle, S., D'Anna, B., Decesari, S., Gilardoni, S., Fischer, M., Fjaeraa, A. M., Fountoukis, C., George, C., Gomes, L., Halloran, P., Hamburger, T., Harrison, R. M., Herrmann, H., Hoffmann, T., Hoose, C., Hu, M., Hyvärinen, A., Hõrrak, U., Iinuma, Y., Iversen, T., Josipovic, M., Kanakidou, M., Kiendler-Scharr, A., Kirkevåg, A., Kiss, G., Klimont, Z., Kolmonen, P., Komppula, M., Kristjánsson, J.-E., Laakso, L., Laaksonen, A., Labonnote, L., Lanz, V. A., Lehtinen, K. E. J., Rizzo, L. V.,

Makkonen, R., Manninen, H. E., McMeeking, G., Merikanto, J., Minikin, A., Mirme, S., Morgan, W. T., Nemitz, E., O'Donnell, D., Panwar, T. S., Pawlowska, H., Petzold, A., Pienaar, J. J., Pio, C., Plass-Duelmer, C., Prévôt, A. S. H., Pryor, S., Reddington, C. L., Roberts, G., Rosenfeld, D., Schwarz, J., Seland, Ø., Sellegri, K., Shen, X. J., Shiraiwa, M., Siebert, H., Sierau, B., Simpson, D., Sun, J. Y., Topping, D., Tunved, P., Vaattovaara, P., Vakkari, V., Veefkind, J. P., Visschedijk, A., Vuollekoski, H., Vuolo, R., Wehner, B., Wildt, J., Woodward, S., Worsnop, D. R., van Zadelhoff, G.-J., Zardini, A. A., Zhang, K., van Zyl, P. G., Kerminen, V.-M., S Carslaw, K., and Pandis, S. N.: General overview: European Integrated project on Aerosol Cloud Climate and Air Quality interactions (EUCAARI) – integrating aerosol research from nano to global scales, Atmos. Chem. Phys., 11, 13061–13143, 2011.

Kurtén, T., Loukonen, V., Vehkamäki, H., and Kulmala, M.: Amines are likely to enhance neutral and ion-induced sulfuric acid-water nucleation in the atmosphere more effectively than ammonia, Atmos. Chem. Phys., 8, 4095–4103, 2008.

Laakso, L., Mäkelä, J. M., Pirjola, L., and Kulmala, M.: Model studies on ion-induced nucleation in the atmosphere, J. Geophys. Res, 107, 4427, doi:10.1029/2002JD002140, 2002.

Laakso, L., Gagné, S., Petäjä, T., Hirsikko, A., Aalto, P. P., Kulmala, M., and Kerminen, V.-M.: Detecting charging state of ultra-fine particles: instrumental development and ambient measurements, Atmos. Chem. Phys., 7, 1333–1345, 2007a.

Laakso, L., Grönholm, T., Kulmala, L., Haapanala, S., Hirsikko, A., Lovejoy, E. R., Kazil, J., Kurtén, T., Boy, M., Nilsson, E. D., Sogachev, A., Riipinen, I., Stratmann, F., and Kulmala, M.: Hot-air balloon as a platform for boundary layer profile measurements during particle formation, Boreal Env. Res., 12, 279–294, 2007b.

Langmann, B., Folch, A., Hensch, M., and Matthias, V.: Volcanic ash over Europe during the eruption of Eyjafjallajökull on Iceland, April–May 2010, Atmos. Environ., 48, 1−8, 2012.

Larriba, C., Hogan, C. J., Attoui, M., Borrajo, R., Garcia, J. F., and de la Mora, J. F.: The Mobility–Volume Relationship below 3.0 nm Examined by Tandem Mobility–Mass Measurement, Aerosol Sci. Tech., 45, 453–467, 2011.

Lee, A. K. Y., Herckes, P., Leaitch, W. R., Macdonald, A. M., and Abbatt, J. P. D.: Aqueous OH oxidation of ambient organic aerosol and cloud water organics: Formation of highly oxidized products, Geophys. Res. Lett., 38, 24, doi:10.1029/2011GL049881, 2011.

Lehtinen, K. E. J., and Kulmala, M.: A model for particle formation and growth in the atmosphere with molecular resolution in size, Atmos. Chem. Phys., 2, 251–257, 2003.

Liu, J., Horowitz, L. W., Fan, S., Carlton, A. G., and Levy, H.: Global in-cloud production of secondary organic aerosols: Implementation of a detailed chemical mechanism in the GFDL atmospheric model AM3, J. Geophys. Res., 117, D15, doi:10.1029/2012JD017838, 2012.

Loukonen, V., Kurtén, T., Ortega, I. K., Vehkamäki, H., Pádua, A. A. H., Sellegri, K., and Kulmala, M.: Enhancing effect of dimethylamine in sulfuric acid nucleation in the presence of water – a computational study, Atmos. Chem. Phys., 10, 4961–4974, 2010.

Lovejoy, E. R., Curtius, J., and Froyd, K. D.: Atmospheric ion-induced nucleation of sulfuric acid and water, J. Geophys. Res., 109, D08204, doi:10.1029/2003JD004460, 2004.

Lushnikov, A. A., and Kulmala, M.: Charging of aerosol particles in the near free-molecule regime, Eur. Phys. J., D 29, 345–355, 2004.

Mäkelä, J. M., Aalto, P., Jokinen, V., Pohja, T., Nissinen, A., Palmroth, S., Markkanen, T., Seitsonen, K., Lihavainen, H., and Kulmala, M.: Observations of ultrafine aerosol particle formation and growth in boreal forest, Geophys. Res. Lett., 24, 10, doi:10.1029/97GL00920, 1997.

Mäkelä, J. M., Salm, J., Smirnov, V. V., Koponen, I., Paatero, J., and Pronin, A. A.: Electrical charging state of fine and ultrafine particles in boreal forest air, J. Aerosol Sci., 32, S149–S150, 2001.

Makkonen, R., Asmi, A., Kerminen, V.-M., Boy, M., Arneth, A., Hari, P., and Kulmala, M.: Air pollution control and decreasing new particle formation lead to strong climate warming, Atmos. Chem. Phys., 12, 1515–1524, 2012.

Manninen, H. E., Nieminen, T., Asmi, E., Gagné, S., Häkkinen, S. K., Lehtipalo, K., Aalto, P., Vana, M., Mirme, A, Mirme, S., Hõrrak, U., Plass-Dülmer, C., Stange, G., Kiss, G., Hoffer, A., Törő, N., Moerman, M., Henzing, B., de Leeuw, G., Brinkenberg, M., Kouvarakis, G. N., Bougiatioti, A., Mihalopoulos, N., O'Dowd, C., Ceburnis, D., Arneth, A., Svenningsson, B., Swietlicki, E., Tarozzi, L., Decesari, S., Facchini, M. C., Birmili, W., Sonntag, A., Wiedensohler, A., Boulon, J., Sellegri, K., Laj, P., Gysel, M., Bukowiecki, N., Weingartner, E., Wehrle, G., Laaksonen, A., Hamed, A., Joutsensaari, J., Petäjä, T., Kerminen, V.-M., and Kulmala, M.:

EUCAARI ion spectrometer measurements at 12 European sites – analysis of new particle formation events, Atmos. Chem. Phys., 10, 7907–7927, 2010.

Martin, S. T., Andreae, M. O., Althausen, D., Artaxo, P., Baars, H., Borrmann, S., Chen, Q., Farmer, D. K., Guenther, A., Gunthe, S. S., Jimenez, J. L., Karl, T., Longo, K., Manzi, A., Müller, T., Pauliquevis, T., Petters, M. D., Prenni, A. J., Pöschl, U., Rizzo, L. V., Schneider, J., Smith, J. N., Swietlicki, E., Tota, J., Wang, J., Wiedensohler, A., and Zorn, S. R.: An overview of the Amazonian Aerosol Characterization Experiment 2008 (AMAZE-08), Atmos. Chem. Phys., 10, 11415–11438, 2010.

McMurry, P. H., and Friedlander, S. K.: New particle formation in the presence of an aerosol, Atmos. Environ., 13, 1635–1651, 1979.

Merikanto, J., Spracklen, D. V., Mann, G. W., Pickering, S. J., and Carslaw, K. S.: Impact of nucleation on global CCN, Atmos. Chem. Phys., 9, 8601–8616, 2009.

Mick., H. J., Hospital, A., and Roth, P.: Computer simulation of sooth particle coagulation in low pressure flames, J. Aerosol Sci., 22, 831–841, 1991.

Mirme, A., Tamm, E., Mordas, G., Vana, M., Uin, J., Mirme, S., Bernotas, T., Laakso, L., Hirsikko, A., and Kulmala, M.: Wide-range multi-channel Air Ion Spectrometer, Boreal Env. Res., 12, 247–264, 2007.

Monge, M. E., Rosenørn, T., Favez, O., Müller, M., Adler, G., Riziq, A. A., Rudich, Y., Herrmann, H., George, C. and D'Anna, B.: Alternative pathway for atmospheric particles growth, P. Natl. Acad. Sci. USA, 109, 6840–6844, 2012.

Nadykto, A. B., and Yu, F.: Uptake of neutral polar vapor molecules by charged clusters/particles: Enhancement due to dipole-charge interaction, J. Geophys. Res., 108, 4717, doi:10.1029/2003JD003664, 2003.

Napari, I., Noppel, M., Vehkamäki, H., and Kulmala, M.: An improved model for ternary nucleation of sulfuric acid – ammonia – water, J. Chem. Phys., 116, 4221–4227, 2002.

Nieminen, T., Lehtinen, K. E. J., and Kulmala, M.: Sub-10 nm particle growth by vapor condensation – effects of vapor molecule size and particle thermal speed, Atmos. Chem. Phys., 10, 9773–9779, 2010.

Nolan, P. J.: The Recombination Law for Weak Ionization, Nature, 148, 26, 1941.

O'Dowd, C. D., Hämeri, K., Mäkelä, J. M., Väkeva, M., Aalto, P. P., de Leeuw, G., Kunz, G. J., Becker, E., Hansson, H.-C., Allen, A. G., Harrion, R. M., Berresheim, H., Kleefeld, C., Geever, M., Jennings, S. G., and Kulmala M.: Coastal new particle formation: Environmental conditions and aerosol physico-chemical characteristics during nucleation bursts, J. Geophys. Res., 107, 10.1029/2000JD000206, 2002.

Ortega, I. K., Kupiainen, O., Kurtén, T., Olenius, T., Wilkman, O., McGrath, M. J., Loukonen, V., and Vehkamäki, H.: From quantum chemical formation free energies to evaporation rates, Atmos. Chem. Phys., 12, 225–235, 2012.

Paasonen, P., Olenius, T., Kupiainen, O., Kurtén, T., Petäjä, T., Birmili, W., Hamed, A., Hu, M., Huey, L. G., Plass-Duelmer, C., Smith, J. N., Loukonen, V., McGrath, M. J., Ortega, I. K., Laaksonen, A., Vehkamäki, H., Kerminen, V.-M., and Kulmala, M.: On the formation of sulphuric acid-amine clusters in varying atmospheric conditions and its influence on atmospheric new particle formation, Atmos. Chem. Phys. Discuss., 12, 11485–11537, 2012.

Peled, R.: Air pollution exposure: Who is at high risk?, Atmos. Environ., 45, 1781–1785, 2011.

Pierce, J. R., and Adams, P. J.: Efficiency of cloud condensation nuclei formation from ultrafine particles, Atmos. Chem. Phys., 7, 1367–1379, 2007.

Pierce, J. R., Riipinen, I., Kulmala, M., Ehn, M., Petäjä, T., Junninen, H., Worsnop, D. R., and Donahue, N. M.: Quantification of the volatility of secondary organic compounds in ultrafine particles during nucleation events, Atmos. Chem. Phys., 11, 9019–9036, 2011.

Pöschl, U.: Atmospheric Aerosols: Composition, Transformation, Climate and Health Effects, Angew. Chem. Int. Ed., 44, 7520–7540, 2005.

Raes, F., Van Dingenen, R., Vignati, E., Wilson, J., Putaud, J.-P., Seinfeld, J. H., and Adams, P.: Formation and cycling of aerosols in the global troposphere, Atmos. Environ., 34, 4215–4240, 2000.

Rannik, Ü., Aalto, P., Keronen, P., Vesala, T., and Kulmala, M.: Interpretation of aerosol particle fluxes over a pine forest: Dry deposition and random errors, J. Geophys. Res., 108, 4544, doi:10.1029/2003JD003542, 2003.

Reischl., G. P., Mäkelä, J. M., Karch, R., and Necid, J.: Bipolar charging of ultrafine particles in the size range below 10 nm, J. Aerosol Sci., 6, 931–949, 1996.

Riipinen, I., Sihto, S.-L., Kulmala, M., Arnold, F., Dal Maso, M., Birmili, W., Saarnio, K., Teinilä, K., Kerminen, V.-M., Laaksonen, A., and Lehtinen, K. E. J.: Connections between atmospheric sulphuric acid and new particle formation during QUEST III–IV campaigns in Heidelberg and Hyytiälä, Atmos. Chem. Phys., 7, 1899–1914, 2007.

Riipinen, I., Pierce, J. R., Yli-Juuti, T., Nieminen, T., Häkkinen, S., Ehn, M., Junninen, H., Lehtipalo, K., Petäjä, T., Slowik, J., Chang, R., Shantz, N. C., Abbatt, J., Leaitch, W. R., Kerminen, V.-M., Worsnop, D. R., Pandis, S. N., Donahue, N. M., and Kulmala, M.: Organic condensation: a vital link connecting aerosol formation to cloud condensation nuclei (CCN) concentrations, Atmos. Chem. Phys., 11, 3865–3878, 2011.

Riipinen, I., Yli-Juuti, T., Pierce, J. R., Petäjä, T., Worsnop, D. R., Kulmala, M., and Donahue, N. M.: The contribution of organics to atmospheric nanoparticle growth, Nat. Geosci., 5, 453–458, 2012.

Seaton, A., MacNee, W., Donaldson, K., and Godden, D.: Particulate air pollution and acute health effects, Lancet, 345, 176–178, 1995.

Seinfeld, J. H., and Pandis, S. N.: Atmospheric Chemistry and Physics: From air Pollution to Climate Change, John Wiley, New York, USA, pp. 1326, 1998.

Sievering, H., Boatman, J., Gorman, E., Kim, Y., Anderson, L., Ennis, G., Luria, M., and Pandis, S.: Removal of sulphur from the marine boundary layer by ozone oxidation in sea-salt aerosols, Nature, 360, 571–573, 1992.

Sihto, S.-L., Kulmala, M., Kerminen, V.-M., Dal Maso, M., Petäjä, T., Riipinen, I., Korhonen, H., Arnold, F., Janson, R., Boy, M., Laaksonen, A., and Lehtinen, K. E. J.: Atmospheric sulphuric acid and aerosol formation: implications from atmospheric measurements for nucleation and early growth mechanisms, Atmos. Chem. Phys., 6, 4079–4091, 2006.

Sipilä, M., Berndt, T., Petäjä, T., Brus, D., Vanhanen, J., Stramann, F., Patokoski, J., Mauldin III, R. L., Hyvärinen, A.-P., Lihavainen, H., and Kulmala, M.: The role of sulfuric acid in atmospheric nucleation, Science, 327, 1243–1246, 2010.

Sorooshian, A., Murphy, S. M., Hersey, S., Bahreini, R., Jonsson, H., Flagan, R. C., and Seinfeld, J. H.: Constraining the contribution of organic acids and AMS m/z 44 to the organic aerosol budget: On the importance of meteorology, aerosol hygroscopicity, and region, Geophys. Res. Lett., 37, L21807, doi:10.1029/2010GL044951, 2010.

Spracklen, D. V., Carslaw, K. S., Kulmala, M., Kerminen, V.-M., Mann, G. W., and Sihto, S.-L.: The contribution of boundary layer nucleation events to total particle concentrations on regional and global scales, Atmos. Chem. Phys., 6, 5631–5648, 2006.

Spracklen, D. V., Carslaw, K. S., Kulmala, M., Kerminen, V.-M., Sihto, S.-L., Riipinen, I., Merikanto, J., Mann, G. W., Chipperfield, M. P., Wiedensohler, A., Birmili, W., and Lihavainen, H.: Contribution of particle formation to global cloud condensation nuclei concentrations, Geophys. Res. Lett., 35, L06808, doi:10.1029/2007GL033038, 2008.

Stolzenburg, M. R., McMurry, P. H., Sakurai, H., Smith, J. N., Mauldin III, R. L., Eisele, F. L., and Clement, C. F.: Growth rates of freshly nucleated atmospheric particles in Atlanta, J. Geophys. Res., 110, D22S05, doi:10.1029/2005JD005935, 2005.

Svensmark, H., and Friis-Christensen, E.: Variation of cosmic ray flux and global cloud coverage—a missing link in solar-climate relationships, J. Atmos. Sol.-Terr. Phys., 59, 1225–1232, 1997.

Tammet, H., Kimmel, V., and Israelsson, S.: Effect of atmospheric electricity on dry deposition of airborne particles from atmosphere, Atmos. Environ., 35, 3423–3419, 2001.

Tammet, H., and Kulmala, M.: Simulation tool for atmospheric aerosol nucleation bursts, J. Aerosol Sci., 36, 173–196, 2005.

Twomey, S.: The influence of pollution on the shortwave albedo of clouds, J. Atmos. Sci., 34, 1149–1152, 1977.

Weber, R. J., Marti, J. J., McMurry, P. H., Eisele, F. L., Tanner, T. J., and Jefferson, A.: Measured atmospheric new particle formation rates: Implications for nucleation mechanisms, Chem. Eng. Commun., 151, 53–64, 1996.

Weber, R. J., Marti, J. J., McMurry, P. H., Eisele, F. L., Tanner, D. J., and Jefferson, A.: Measurements of new particle formation and ultrafine particle growth rates at a clean continental site, J. Geophys. Res., 102, D4, 4375–4385, doi:10.1029/96JD03656, 1997.

Weber, R. J., Moore, K., Kapustin, V., Clarke, A., Mauldin, R. L., Kosciuch, E., Cantrell, C., Eisele, F., Anderson, B., and Thornhill, L.: Nucleation in the equatorial Pacific during PEM-Tropics B: Enhanced boundary layer H_{2SO4} with no particle production, J. Geophys. Res., 106, D32, doi:10.1029/2001JD900250, 2001.

WHO: Global health risks: mortality and burden of disease attributable to selected major risks, WHO Press, Geneva, Switzerland, 2004.

Wiedensohler, A.: An approximation of the bipolar charge distribution for particles in the submicron range, J. Aerosol Sci., 19, 387–389, 1988.

Winkler, P. M., Steiner, G., Virtala, A., Vehkamäki, H., Noppel, M., Lehtinen, K. E. J., Reischl, G. P., Wagner, P. E., and Kulmala, M.: Heterogeneous Nucleation Experiments Bridging the Scale from Molecular Ion Clusters to Nanoparticles, Science, 319, 1374, 2008.

Yli-Juuti, T., Nieminen, T., Hirsikko, A., Aalto, P. P., Asmi, E., Hõrrak, U., Manninen, H. E., Patokoski, J., Dal Maso, M., Petäjä, T., Rinne, J., Kulmala, M., and Riipinen, I.: Growth rates of nucleation mode particles in Hyytiälä during 2003–2009: variation with particle size, season, data analysis method and ambient conditions, Atmos. Chem. Phys., 11, 12865–12886, 2011.

Yu, F., and Turco, R.: Case studies of particle formation events observed in boreal forests: implications for nucleation mechanisms, Atmos. Chem. Phys., 8, 6085–6102, 2008.

Yu, F., Luo, G., Bates, T. S., Anderson, B., Clarke, A., Kapustin, V., Yantosca, R. M., Wang, Y., and Wu, S.: Spatial distributions of particle number concentrations in the global troposphere: Simulations, observations, and implications for nucleation mechanisms, J. Geophys. Res., 115, D17205, doi:10.1029/2009JD013473, 2010.

Yu, F.: A secondary organic aerosol formation model considering successive oxidation aging and kinetic condensation of organic compounds: global scale implications, Atmos. Chem. Phys., 11, 1083–1099, 2011.

Zhang, K. M., and Wexler, A. S.: A hypothesis for growth of fresh atmospheric nuclei, J. Geophys. Res., 107, 4577, doi:10.1029/2002JD002180, 2002.

Zhang, R., Khalizov, A., Wang, L., Hu, M. and Xu, W.: Nucleation and Growth of Nanoparticles in the Atmosphere, Chem. Rev., 112, 1957–2011, 2012.